Topics in Current Chemistry Collections

Youhong Tang
Ben Zhong Tang *Editors*

Aggregation-Induced Emission

Springer

Topics in Current Chemistry Collections

Aims and Scope

The series *Topics in Current Chemistry Collections* presents critical reviews from the journal *Topics in Current Chemistry* organized in topical volumes. The scope of coverage is all areas of chemical science including the interfaces with related disciplines such as biology, medicine and materials science.

The goal of each thematic volume is to give the non-specialist reader, whether in academia or industry, a comprehensive insight into an area where new research is emerging which is of interest to a larger scientific audience.

Each review within the volume critically surveys one aspect of that topic and places it within the context of the volume as a whole. The most significant developments of the last 5 to 10 years are presented using selected examples to illustrate the principles discussed. The coverage is not intended to be an exhaustive summary of the field or include large quantities of data, but should rather be conceptual, concentrating on the methodological thinking that will allow the non-specialist reader to understand the information presented.

Contributions also offer an outlook on potential future developments in the field.

More information about this series at http://www.springer.com/series/14181

Youhong Tang • Ben Zhong Tang
Editors

Aggregation-Induced Emission

With contributions from

Alessandro Aliprandi • Luisa De Cola • Jun Dai • Lei Dong
Suzanne Fery-Forgues • Amin Jamshidi Ghahfarokhi • Ting Han
Jing-Jing Hu • Vishal Kachwal • Inamur Rahaman Laskar
Dangyuan Lei • Siqi Li • Xiaoding Lou • Fan Luo • Dongge Ma
Guillermo Moreno-Alcántar • Li-Ya Niu • Hui-Qing Peng
Harini A. Perera • Ana Clara B. Rodrigues • J. Sérgio Seixas de Melo
Ben Zhong Tang • Youhong Tang • Javad Tavakoli
Corinne Vanucci-Bacqué • Dong Wang • Xinnan Wang
Zhaoyu Wang • Jiaming Wei • Fan Xia • Mingdi Yan
Juliang Yang • Qing-Zheng Yang • Ruquan Ye • Haoke Zhang

Springer

Editors
Youhong Tang
College of Science and Engineering
Flinders University
Adelaide, SA, Australia

Ben Zhong Tang
School of Science and Engineering
The Chinese University of Hong Kong
Shenzhen, China

Partly previously published in Topics in Current Chemistry Volume 378 (2020); Topics in Current Chemistry Volume 379 (2021).

ISSN 2367-4067
Topics in Current Chemistry Collections
ISBN 978-3-030-89932-5

© The Editor(s) (if applicable) and The Author(s), under exclusive license to Springer Nature Switzerland AG 2022
Chapter "Aggregation-Induced Emission In Electrochemiluminescence: Advances and Perspectives" is licensed under the terms of the Creative Commons Attribution 4.0 International License (http://creativecommons.org/licenses/by/4.0/). For further details see license information in the chapters.
This work is subject to copyright. All rights are solely and exclusively licensed by the Publisher, whether the whole or part of the material is concerned, specifically the rights of translation, reprinting, reuse of illustrations, recitation, broadcasting, reproduction on microfilms or in any other physical way, and transmission or information storage and retrieval, electronic adaptation, computer software, or by similar or dissimilar methodology now known or hereafter developed.
The use of general descriptive names, registered names, trademarks, service marks, etc. in this publication does not imply, even in the absence of a specific statement, that such names are exempt from the relevant protective laws and regulations and therefore free for general use.
The publisher, the authors, and the editors are safe to assume that the advice and information in this book are believed to be true and accurate at the date of publication. Neither the publisher nor the authors or the editors give a warranty, expressed or implied, with respect to the material contained herein or for any errors or omissions that may have been made. The publisher remains neutral with regard to jurisdictional claims in published maps and institutional affiliations.

This Springer imprint is published by the registered company Springer Nature Switzerland AG
The registered company address is: Gewerbestrasse 11, 6330 Cham, Switzerland

Contents

Preface

Aggregation-induced emission (AIE) is a new branch of luminescent materials research that aims to explore luminescence at the aggregate level. AIE luminogens (AIEgens) often show no emission in solutions at the molecular level but become brightly emissive when their molecular species are aggregated. Aggregation processes generally involve the interplay of competitive or cooperative effects, and new structures, properties, and functions usually appear and diversify in the aggregates. Over the course of the last 20 years, AIE research has made great strides in material development, mechanistic study, and high-tech applications. Meanwhile, research on AIE is an ideal entry point for scientists to explore and unravel the mysteries in the meso world, since AIE is a typical phenomenon showing a nonlinear property change from molecules to aggregates. The past two decades has witnessed booming progress in AIE research. Some examples of the remarkable advances in the field of AIE study in recent years are presented in this topical collection.

Niu *et al.* summarize recent progress in the design strategy of AIE-based energy transfer systems for light-harvesting, fluorescent probes and theranostic systems, with an emphasis on design strategies to achieve desirable properties. The limitations, challenges, and future opportunities of AIE-excitation energy transfer systems are briefly outlined. The discovery of aggregation-induced electrochemiluminescence (AIECL) in 2017 has opened new research avenues in the quest for novel, more efficient emitters and offered platforms for biological and environmental sensing applications. The great abundance of fluorophores presenting AIE in aqueous media renders AIECL a potentially powerful tool for future diagnostics. De Cola *et al.* give their reflections about the future directions to take for the development of sensing devices based on AIECL. Ye *et al.* highlight recent developments in clusteroluminescence, including mechanistic studies, the disclosure of room-temperature phosphorescence, and the extension of light emission to the longer-wavelength region and also demonstrate a few applications in various fields. Kachwal and Laskar review AIE-active organic mechanofluorochromic materials, i.e., AIEgens with changes in their emissions under anisotropic and isotropic pressures. The relationship between the chemical structures of AIEgens and the change in the emission behaviours under pressures is discussed.

Fery-Forgues and Vanucci-Bacqué encompass the various ways to use benzazole units in solid-state luminescence enhancement systems. They underline the significant progress recently made in the understanding of the photophysical mechanisms involved. Benzazoles are robust building blocks, easily incorporated into a variety of structures which demonstrates advantages taken from these small heterocycles for the design of increasingly efficient AIEgens. Ma reviews the status and envisions the prospects of AIEgens in organic light-emitting diodes, optically pumping organic lasers, organic solar cells and organic photodetectors. It demonstrates that AIEgens are important organic optoelectronic materials.

The enhancement of photoluminescence through formation of molecular aggregates in organic oligomers and conjugated organic polymers is reviewed by Rodrigues and de Melo. Future perspectives for the rational design of AIEgen structures are discussed. Fluorescent gels have numerous properties that are intrinsic to the gel structures, with additional light-emitting properties making them attractive for different applications. Y Tang *et al.* summarize current studies associated with the development of fluorescent gels using AIEgens and propose new directions for future research, especially the biomedical applications in drug delivery, biosensors, bioimaging, and tissue engineering. B Z Tang *et al.* review the recent advances in the design, preparation, performance, and applications of functional synthetic polymer systems with AIE attribute and stimuli responses. Various AIE-based polymer systems responding to single or multiple physical or chemical stimuli are illustrated with specific examples. The current challenges and perspectives on the future development of this research area are also discussed.

Enzyme-responsive peptide-based AIE bioprobes used for biomedical applications are summarized by Lou *et al.* How each aggregation strategy detects enzyme activity and treats the diseases under imaging guidance are discussed and the current problems and future prospects of enzyme-responsive peptide-based AIE bioprobes are explored in this review. Perera and Yan highlight examples where AIEgens are employed as molecular probes in the imaging, discrimination and killing of bacteria, viruses and fungi.

As guest editors, we are sincerely thankful for the great contributions from all the authors and the professional assistance from the editorial office of *Topics in Current Chemistry*. We hope this topical collection will attract broad attention among scientists and technologists and inspire scientific exploration at the aggregate level and high-tech innovation utilizing AIEgens.

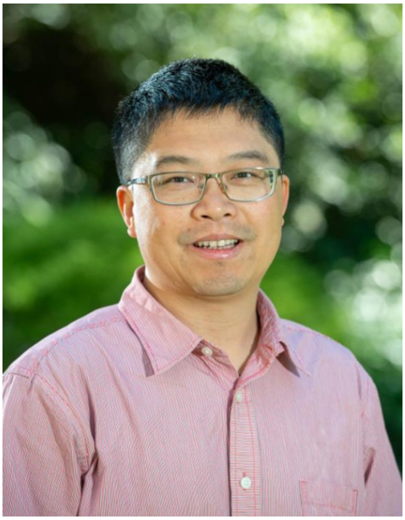

Youhong Tang
College of Science and Engineering
Flinders University, Australia

Ben Zhong Tang
School of Science and Engineering
The Chinese University of Hong Kong, Shenzhen, China

Topics in Current Chemistry (2021) 379:15
https://doi.org/10.1007/s41061-021-00327-9

REVIEW

Aggregation-Induced Emission: From Small Molecules to Polymers—Historical Background, Mechanisms and Photophysics

Ana Clara B. Rodrigues[1] · **J. Sérgio Seixas de Melo**[1]

Received: 2 January 2021 / Accepted: 12 February 2021 / Published online: 16 March 2021

Abstract

The enhancement of photoluminescence through formation of molecular aggregates in organic oligomers and conjugated organic polymers is reviewed. A historical contextualization of aggregation-induced emission (AIE) phenomena is presented. This includes the loose bolt or free rotor effect and J-aggregation phenomena, and discusses their characteristic features, including structures and mechanisms. The basis of both effects is examined in key molecules, with a particular emphasis on the AIE effect occurring in conjugated organic polymers with a polythiophene (PT) skeleton with triphenylethylene (TPE) units. Rigidification of the excited state structure is one of the defining conditions required to obtain AIE, and thus, by changing from a flexible ground state to rigid (quinoidal-like) structures, oligo and PTs are among the most promising emerging molecules alongside with the more extensively used TPE derivatives. Molecular structures moving away from the domination of aggregation-caused quenching to AIE are presented. Future perspectives for the rational design of AIEgen structures are discussed.

Keywords AIE · Organic conjugated polymers · Polythiophenes · J-aggregates · Fluorescence

---

Chapter 7 was originally published as Rodrigues, A. C. B. & Seixas de Melo, J. S. Topics in Current Chemistry (2021) 379: 15. https://doi.org/10.1007/s41061-021-00327-9.

✉ J. Sérgio Seixas de Melo
ana.beltran@uc.pt; sseixas@ci.uc.pt

[1] Department of Chemistry, Coimbra Chemistry Centre, University of Coimbra, 3004-535 Coimbra, Portugal

1 Background to the AIE Phenomena: An Historical Perspective

Already 20 years have passed since Tang et al. [1] reported a system that, in 2001, introduced the concept of aggregation-induced emission (AIE) in contrast to the most common opposing phenomenon of quenching of fluorescence occurring in the great majority of fluorophores in solid state as a result of aggregation-caused quenching (ACQ) [2]. Tang et al. pioneered these studies, reporting on the efficient blue emission of 1-methyl-1,2,3,4,5-pentaphenylsilole in thin films, which, upon addition of water (a poor solvent), were shown to induce aggregate formation on these silole derivatives in ethanolic solution [1, 3].

Before the findings Tang et al., there had been only a few reports on enhanced emission in the solid state [4]; these included the enhancement of phosphorescence emission in xanthene dyes (eosin and erythrosine) in mixture of glycerol:water frozen glass [5], excimer emission of hydrocarbons in restricted molecular arrangements [6, 7] and in poor solvent medium [8], and emission of J-aggregates formed in pyridinium-substituted indolizines [9] and in cyanine and merocyanine dyes (Scheme 1) [10, 11]. However, emission enhancement in aggregates, with a new fluorescence band associated with intermolecular interactions, had been reported in the first half of the twentieth century.

1.1 Enhancement of Emission from J-Aggregate Formation

In 1936, Scheibe 12] and Jelley [13, 14] independently observed an unusual behaviour of pseudoisocyanine chloride [also known as 1,1′-diethyl-2,2′-cyanine chloride, PIC chloride (Scheme 1)]: in aqueous solution, the absorption maximum of the spectrum shifted to lower energies (red-shift) when compared with the spectrum of the same dye in ethanol; upon increase of the dye concentration in water this band became more intense and sharp [15]. Dye aggregates with a narrow absorption band that is shifted to longer wavelengths (bathochromically shifted), with very small Stokes shift and increased fluorescence intensity relative to the monomer, are generally designated as Scheibe aggregates or J-aggregates (J denotes Jelley after its discoverer) [11, 16]. In contrast, aggregates with absorption bands shifted to shorter wavelengths (hypsochromically shifted) with respect to the monomer band are designated H-aggregates (H denotes hypsochromic) and exhibit, in most cases, low or almost total absence of fluorescence [17]. The mechanisms associated with these interactions are better understood with the Exciton Model of Kasha, but are out of the scope of this review [16, 18, 19]. The AIE effect partially contrasts with the formation of emissive H- (non-emissive) or J- (emissive) aggregates because AIE interaction of two molecules leads to a rigidification of the molecular structure—not mandatory in J-aggregates—thus decreasing the efficiency of the radiationless internal conversion channel and increasing the efficiency of the radiative de-excitation channel.

Enhancement of emission caused by J-aggregates has been described in several systems (Scheme 1). Oelkrug et al. [20] showed the role of J-aggregation in

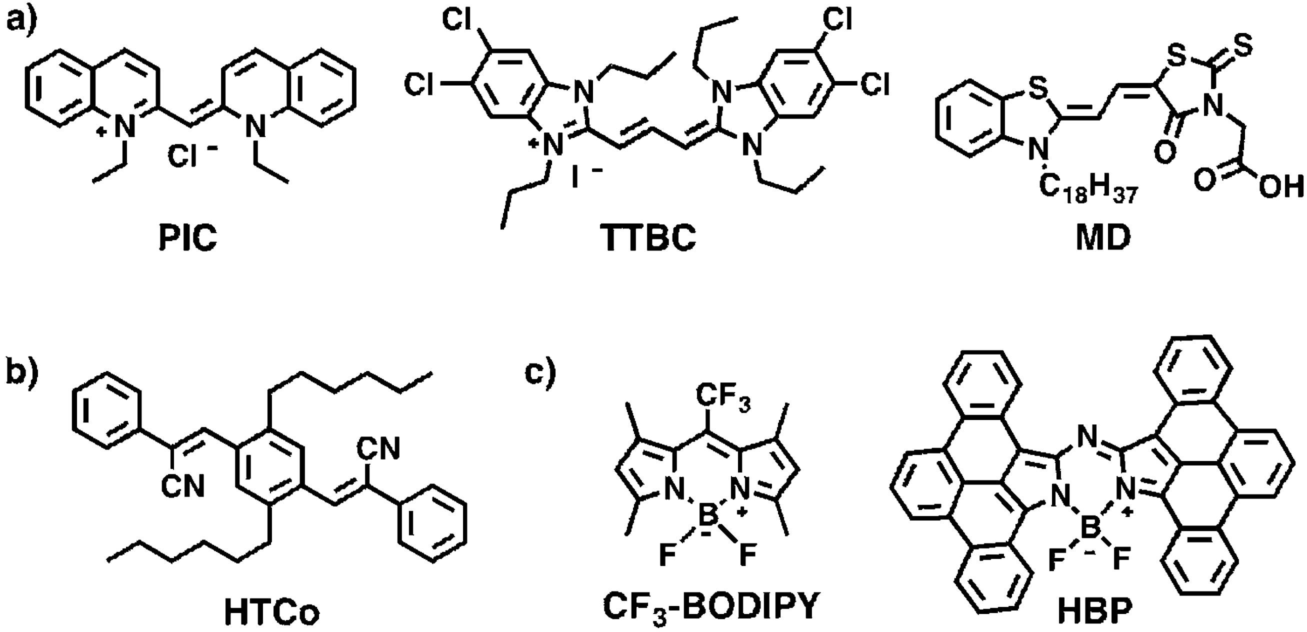

Scheme 1 **a–c** Structures of compounds reported to form emissive J-aggregates. **a** Cyanine and merocyanine derivatives such as 1,1′-diethyl-2,2′-cyanine chloride (PIC chloride); 1,1′,3,3′-tetraethyl-5,5′,6,6′-tetrachlorobenzimidazolocarbocyanine iodide (TTBC iodide) and (3-carboxymethyl-5-[2-(3-octadecyl-2-benzothiazolinylidene) ethylidene]-2-thioxo-4-thiazolidinone (MD). **b** Oligophenylenevinylenes, such as 1,4-bis(α-cyanostyryl)-2,5-di-*n*-hexylbenzene (HTCo). **c** 4,4-Difluoro-4-bora-3a,4a-diaza-s-indacene (BODIPY) systems: CF_3-BODIPY and hexaphenylazaBODIPY (HPB), which are recently reported aggregation-induced emission (AIE)-luminogens

enhancement of emission in solid state oligophenylenevinylenes, with a change in fluorescence quantum yield from practically zero in solution to 60% in nanoparticles or in films, further justifying this phenomenon as arising from the rigid environments provided by viscous solvents, or solid state phases, suppressing the torsion-induced molecular movement associated with nonradiative deactivation [21]. Reports on the formation of J-aggregates in BODIPY systems (4,4-difluoro-4-bora-3a,4a-diaza-s-indacene), and consequently the observation of AIE or aggregation-induced emission enhancement (AIEE) phenomena, were described by Choi et al. [22] with meso-BODIPY derivatives and, more recently, by Sheng et al. [23] in aza-BODIPY. In these works, the substituents were chosen for their proper molecular packing into a J-aggregate structure.

1.2 Monomer-Like Emission Enhancement: The "Loose Bolt" or "Free Rotor" Effect

The AIE-luminogen systems first described by Tang et al. [1, 3, 24–26] resulted from intramolecular rigidification as a consequence of intermolecular interaction [27], but, contrary to J-aggregates, show essentially monomer-like emission [28]. Indeed, the AIE effect results mainly from rigidification of the monomer unit, as a result of this (aggregate) interaction.

In general, rigid systems such as polyaromatic hydrocarbons (PAH) display photoluminescence quantum yields higher than their polyene counterparts (identical or similar number of carbon atoms). Although the emission of PAH depends on symmetry considerations (with the relative position of the two lowest singlet lying states having a determinant role), the presence of heteroatom(s), and solvent (polarity and viscosity), they are most often fluorescent compounds. In a simplified view, this can be attributed to the rigid structure of PAH, which contrasts with the degree of freedom of polyenes or other flexible structures [29]. Several examples, some given in Scheme 2, illustrate this molecular rigidity in comparison with flexible analogues. In Scheme 2, the left hand panel corresponds to rigid structures, all with high fluorescence emission efficiency, whereas the right hand panel depicts "flexible" molecular structures ("rotors"), with poor luminescence quantum yields and, generally, high radiationless internal conversion (S_1~~⟶S_0) deactivation. In the examples given, the twisting motion associated with the skeleton with the double bond(s) becomes locked, and an analogy with the "free rotor" effect, which is now precluded, seems adequate.

In Scheme 2, the structural comparisons can be envisaged as follows. With azabenzene (AB), with $\phi_F \approx 0$, simple blocking of the twisting motion leads to the 9,10-diazaphenanthrene (DPA) structure, now with a $\phi_F = 0.02$ in ethanol and a lifetime of 4.27 ns [30]. With the E- and Z-stilbene structures (the Z-cis structure photoisomerizes in a barrierless process compared with the E-trans structure) [31, 32], which are basically known to be poorly fluorescent at room temperature (with values of $\phi_F = 0.04$–0.05, but temperature dependent and at T = 83.2 K—another way to rigidify the molecular structure—with $\phi_F \sim 0.95$ [33]) can, again by blocking the twisting motion associated with the central double bond, lead to the structures Ind-Ind (indeno[2,l-a]indene) and DPCB (1,2-diphenylcyclobutene), which are

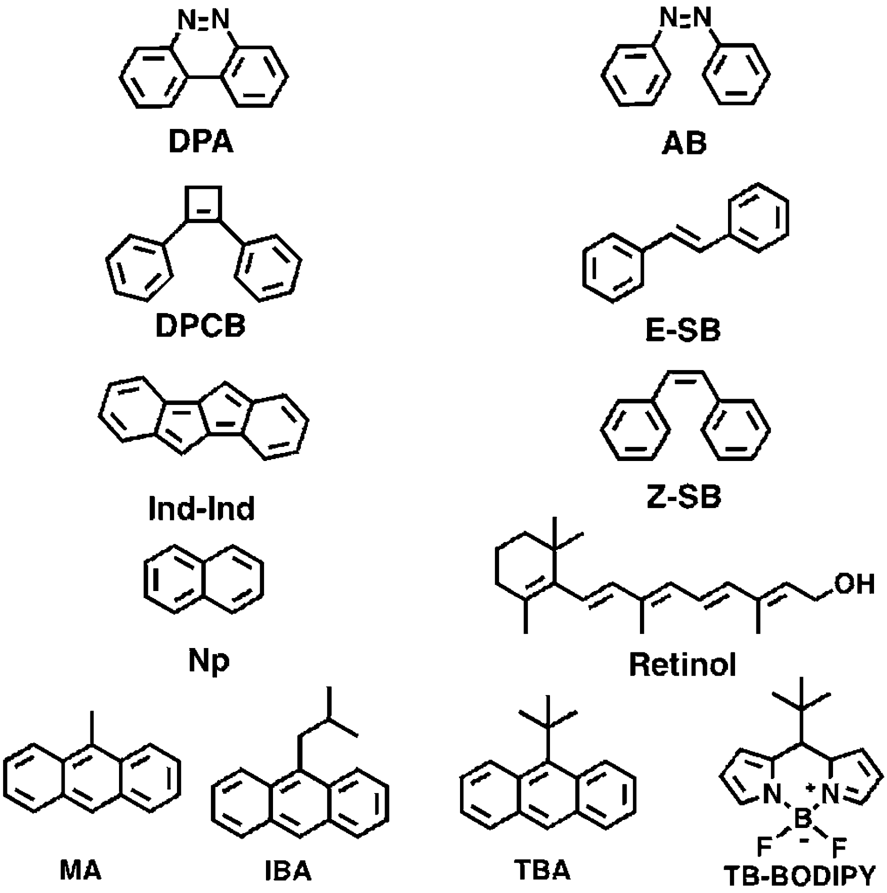

Scheme 2 Structures of compounds with similar structures but that differ in the molecular rigidity and flexibility imparted by C=C bond(s). *DPA* 9,10-diazaphenanthrene, *AB* azabenzene, *DPCB* 1,2-diphenylcyclobutene, *E-SB* trans- or E-stilbene, *Z-SB* cis- or Z-stilbene, I*nd-Ind* *in*deno[2,l-a]indene, *Np* naphthalene, *retinol* (one of the structures of Vitamin A), *MA* 9-methyl-anthracene, *IBA* 9-isobutyl-anthracene, *TBA* 9-(tert-butyl)anthracene, *TB-BODIPY* meso-tert-butyl BODIPY

highly fluorescent with almost unitary ϕ_F values [34, 35]. In Scheme 2, the naphthalene and retinol pair constitutes another classical example where molecules with the same number of carbon–carbon double bonds have differences of almost one order of magnitude in ϕ_F (Np, $\phi_F = 0.21$ [36] in ethanol and retinol with $\phi_F = 0.0298$ in hexane [37], the two obtained at $T = 293$ K), again due to rigidity associated to Np and not present in retinol. There is an additional type of molecule, the 9-alkyl-substituted anthracenes, where this rotor or loose bolt effect is particular notorious and imparts a gain in rigidity of the molecules, in particular, when a comparison of the emission efficiency is made at room temperature between 9-methyl-anthracene (MA, $\phi_F = 0.29$), 9-isobutyl-anthracene (IBA, $\phi_F = 0.39$) and 9-(*tert*-butyl) anthracene (TBA, $\phi_F = 0.011$ in *n*-hexane) [38, 39]. The two structures (MA and

TBA) possess the same chromophoric core (anthracene) and therefore it is not fluorescence deactivation (and associated radiative rate constant) that explains the difference in behavior. Moreover, since triplet formation is found non-populated for 9-(*tert*-butyl)anthracene [39], the large difference between the methyl and tert-butyl derivatives is found in the large increase in the internal conversion deactivation in this latter anthracene derivative. This is a consequence of the fact that the process of converting electronic energy into vibrational energy (from $S_1 \sim\sim\rightarrow S_0$) is much more efficient with the *t*-butyl-anthracene derivative, where there are many more low-lying vibrational modes, to absorb this excess energy, than with the methyl derivative. This increase in size of the substituent augments the number of degrees of vibrational freedom of the molecule, and the energy released through internal conversion turns out to be more efficient at the expense of fluorescence emission (the triplet state formation is inoperative). That is, the loose bolt or rotor effect is more effective with 9-(*tert*-butyl)anthracene. An identical effect is seen with other structures such as the meso-tert-butyl BODIPY, where a S_1/S_0 conical intersection favors the radiationless deexcitation pathway to the ground state [40]. Recent studies comparing flexible versus more rigid similar structures (see Fig. 1 and associated discussion below), point out the relevance of this structural balance in the discussion of the AIE effect [41].

2 Development of AIE-Active Luminogen Molecules

After the account of AIE in pentaphenylsilole [1, 3], another fluorogen found to display this effect was 1,1,2,2-tetraphenylethylene (TPE), again reported by Tang et al. [42]. Although TPE emission has been known for about 50 years [43], in contrast with the poorly emissive E- and Z-stilbenes (Scheme 2), it was with the discovery by Tang of augmented fluorescence emission of this compound in the crystal and in water:acetonitrile mixtures that this effect began to be deeply explored.

The π twist of the central C=C bond of TPE in the excited state [44–46], and the viscosity-dependent fluorescence enhancement [47, 48] were reported in the 1980s and, by the end of the 1990s, several groups had studied these properties using ultrafast spectroscopy methods [49–51]. The origin of AIE phenomena in TPE is likely to be associated with the loose bolt or free rotor effect [52]. This basically leads to an increase (or decrease) of the coupling modes of the vibronic transitions [52, 53]. In systems where there is the possibility of changing from a C=C double bond to a carbon–carbon bond with partial single bond character (upon excitation), this “loose bolt effect” may therefore be considered as the genesis of the AIE effect. Indeed, most initial compounds showing AIE were based on a TPE central core, i.e., there was, in the excited state, a rigidification of these TPE-like molecules, resulting from aggregate interaction, with a decrease in the radiationless internal conversion decay pathway. Actually, this intermolecular interaction involving TPE molecules would result not in a particular emissive aggregate, as with J-aggregates, but in a structural rigidification of the molecule (in the aggregate state) that would preclude the “loose

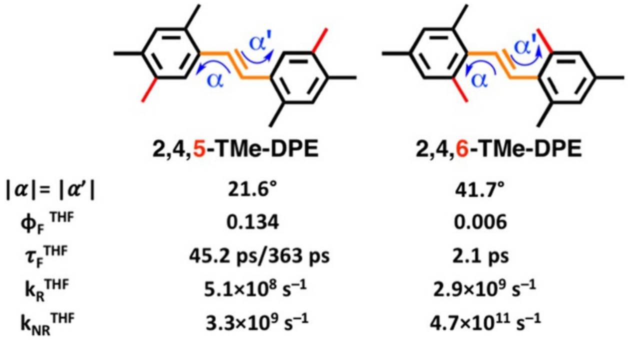

	2,4,5-TMe-DPE	2,4,6-TMe-DPE
$\lvert\alpha\rvert = \lvert\alpha'\rvert$	21.6°	41.7°
ϕ_F^{THF}	0.134	0.006
τ_F^{THF}	45.2 ps/363 ps	2.1 ps
k_R^{THF}	5.1×10^8 s^{-1}	2.9×10^9 s^{-1}
k_{NR}^{THF}	3.3×10^9 s^{-1}	4.7×10^{11} s^{-1}

Fig. 1 Structures of 2,4,5-TMe-DPE and 2,4,6-TMe-DPE along with their photophysical data measured in tetrahydrofuran (THF) solution. ϕ_F Fluorescence quantum yield of solution, τ_F fluorescence decay times, k_R radiative rate constant, k_{NR} nonradiative rate constant [41]

bolt effect" and therefore the "movement" otherwise associated with this highly efficient internal conversion radiationless deactivation.

The pioneering studies of Tang et al. led to a rapid increase in the number of known luminogens with AIE characteristics (AIEgens) [54, 55] and innumerable AIE materials have been developed [56–58]. Other systems with AIE properties have been rediscovered [e.g., AIE building blocks of quinoline-malonitrile (QM) and polyaryl-substituted pyrrole (PAP) in Scheme 3] [54, 59–62]. To design and rediscover new AIEgen molecules it is therefore of utmost relevance to equate the mechanisms leading to the occurrence of AIE and AIEE. The free rotor or loose bolt effect associated with the introduction of the tert-butyl group (or similar groups with a high number of low-lying vibrational modes) will be of relevance in the design of AIE active polymers described in the section on Design and photophysical studies of AIE-active polymers, and is particularly relevant in the section on TPE-based conjugated polymers where a tert-butyl derivative increases its photoluminescence yield in the solid state and in a solvent mixture where a bad solvent (water) is dominant.

2.1 AIE Working Mechanisms

The working mechanisms of AIE have been investigated extensively [63–65]. One such proposed mechanism is restriction of the intramolecular rotation (RIR) [66], which can be measured through temperature-, viscosity-, and intramolecular-steric-hindrance-dependent luminescence quantum efficiency. Restriction of intramolecular vibration (RIV) [67] was also proposed to account for the strong luminescence in the solid state. A more generalized mechanistic model for AIE was proposed by combining RIR and RIV into a global principle of restriction of intramolecular motions (RIM) [68]. Photocyclization [69–71], suppression of the formation of twisted intramolecular charge transfer state [63, 72–74] and Z/E isomerization [75–77] were other hypotheses proposed to explain the occurrence of AIE. RIM was shown to be the main mechanistic cause for AIE effects observed in many luminogen systems based on pure aromatic molecular rotors such as hexaphenylsilole

(HPS). With TPE, recent studies and interpretations favor both RIM [68] and Z/E isomerization [77] being involved in the emission quenching of TPE in solution. Therefore, blocking or limiting these two mechanisms, by aggregate interaction, will lead to AIE. Nevertheless, this topic is still under debate, particularly regarding which molecular mechanism (RIM or isomerization) plays the major role in the AIE effect [78].

Analysis of the potential energy surfaces (PES) of model propeller-shaped structure also showed that the enhancement of emission in the solid state can be associated with the decrease of the excited state decay caused by nonradiative mechanisms [79]. Moreover, computational theoretical studies indicate that the increase of steric hindrance improves the fluorescence quantum efficiency and that rotation of aromatic substituents and π–π stacking interactions are the dominant pathways for the nonradiative decay of AIEgens [80]. Furthermore, the combination of ultrafast photophysical techniques, quantum chemistry calculations and strategic design of new molecules led to three additional proposed AIE mechanisms: restriction of the excited-state “double-bond” torsion (ESDBT) [41], restriction access to conical intersection (RACI) [81, 82] and dark state in heteroatoms systems (RADS) [83].

2.1.1 Stilbene-Like Molecules

Aiming to shed light on the potential reasons why some stilbene-like molecules are emissive in solution, whereas other are not, photophysical studies of two model stilbene derivatives, di-*o*-methyl substituted 2,4,6-TMe-DPE and mono-*o*-methyl substituted 2,4,5-TMe-DPE, were recently conducted [41]. While the twisted structure of 2,4,6-TMe-DPE, which exhibits an AIE effect, was poorly fluorescent in tetrahydrofuran (THF), with a fluorescence quantum yield, $\phi_F = 0.006$, 2,4,5-TMe-DPE, a structurally planar molecule, displayed $\phi_F = 0.134$ in the same solvent (Fig. 1) [41]. Femtosecond transient absorption (fs-TA) measurements for these two molecules in THF showed that two processes are involved in the excited-state deactivation of 2,4,5-TMe-DPE, highlighted by the two time constants ($\tau_1 = 45.2$ ps and $\tau_2 = 363$ ps), while a much faster process occurs with 2,4,6-TMe-DPE ($\tau = 2.1$ ps). The data also indicated that the twisted 2,4,6-TMe-DPE displays a faster excited-state molecular motion than the structurally planar 2,4,5-TMe-DPE ($k_{NR} = 4.7 \times 10^{11}$ s^{-1} vs. 3.3×10^9 s^{-1}), thus showing the clear dominance of the radiationless decay pathways with 2,4,6-TMe-DPE. The restricted molecular motion in the planar 2,4,5-TMe-DPE made the radiative decay comparable with the nonradiative decay, thus clarifying the $\phi_F = 0.134$ obtained in solution.

2.1.2 Quantum Mechanical Calculations

Time-dependent density functional theory (TDDFT) quantum mechanical theory was used to perform calculations in the excited state of 2,4,6-TMe-DPE and 2,4,5-TMe-DPE [41]. The authors concluded that most of the excited state energy of 2,4,6-TMe-DPE was released nonradiatively via the excited-state “double-bond” torsion (ESDBT) mechanism; however, ESDBT was suppressed in 2,4,5-TMe-DPE, and this justified its higher radiative rate constant value, k_R (see Fig. 1) [41].

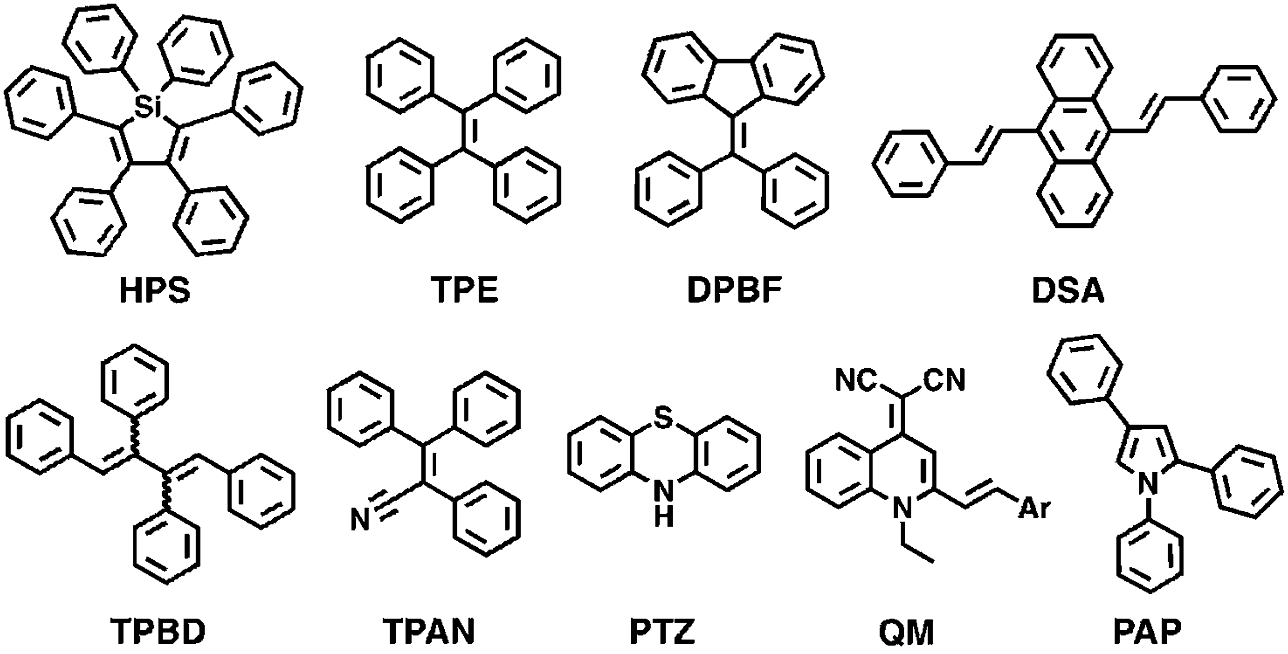

Scheme 3 Molecular structure of some AIE-active luminogen cores. *HPS* Hexaphenylsilole; *TPE* tetraphenylethene; *DPBF* diphenylbenzofulvene; *DSA* 9,10-distyrylanthracene; *TPBD* tetraphenyl-1,4-butadiene; *TPAN* triphenylacrylonitrile; *PTZ* phenothiazine; *QM* quinoline-malonitrile; *PAP* polyaryl-substituted pyrrole

In order to further understand the relationship between intramolecular motions and AIE properties, Blancafort and Morokuma conducted independent quantum chemical investigations [81, 84–86]. They analyze the deactivation processes of AIEgens DPBF [85] , tetraphenylsilole [86], and phenyleneimide [87] with the RACI (restricted access to a conical intersection) model. The RACI model explains the AIE effect by differences in the radiationless decay rate. Their results predicted a largely distorted structure near the minimum energy conical intersection (MECI). In solution, the MECI is easy to access, which contrasts with the solid state situation, where it becomes difficult to access, and it is prohibited in the crystalline state. Later, by studying different substituted TPE derivatives, Kokado et al. [82, 88] indicated that the C=C twist in the excited state is critical in the occurrence of the AIE phenomenon.

Many of these mechanistical studies were performed to specify the exact motions and decay pathways, making the meaning of RIM more accurate and detailed. However, the behavior of heteroatom-containing AIEgens may not be fully explained by RIM. Indeed, for example, a molecule can change its photophysical behavior from AIE to ACQ characteristics, simply by changing a single heteroatom [89, 90]. Two excited states must be taken into account, and a mechanism, restriction of access to dark state (RADS), is specified to fully equate (in addition to RIM) the complete the picture of AIE mechanism. To probe this concept, a nitrogen-containing AIEgen named 9-anthyl-methyl)bis (2-pyridylmethyl)amine (APA in Fig. 2) was chosen as a model compound [83].

From solution to aggregate suspension and then to crystal, the degree of molecular freedom gradually decreases, concomitantly with the increase in ϕ_F (from 0.006 in solution to 0.39 in the crystal) [83]. Also, the radiationless rate constant, k_{NR}, decreases dramatically (103 times higher in solution than in the crystal) while the radiative rate constant, k_R, increases more slightly (by a factor of 15) [83]. These results are in agreement with commonly reported RIM results [68]. Surprisingly, the zinc-APA complex shows not only a drastic decrease in k_{NR} (ca. four orders of magnitude, 5247 higher in solution of the monomer than the complex), but also an enhancement of k_R with $\phi_F = 0.998$ [83]. This has led to the conclusion that RIM and the availability of lone pairs (to establish n,π* transitions) may both influence the emission process [83]. Two possible competing decay pathways may be involved: (1) relaxation to the S_1 to reach the emissive (π,π*); and (2) relaxation to a

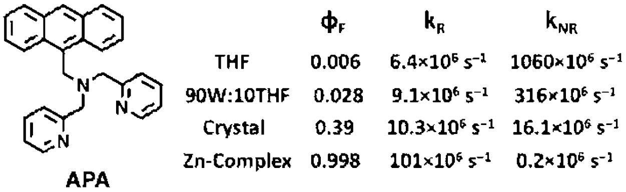

	Φ_F	k_R	k_{NR}
THF	0.006	$6.4\times10^6\ s^{-1}$	$1060\times10^6\ s^{-1}$
90W:10THF	0.028	$9.1\times10^6\ s^{-1}$	$316\times10^6\ s^{-1}$
Crystal	0.39	$10.3\times10^6\ s^{-1}$	$16.1\times10^6\ s^{-1}$
Zn-Complex	0.998	$101\times10^6\ s^{-1}$	$0.2\times10^6\ s^{-1}$

Fig. 2 Structures of 9-anthyl-methyl)bis (2-pyridylmethyl)amine (APA) and photophysical data obtained in THF, 90%water:10% THF (90 W:10THF) mixture, in crystal, and with the Zn-APA complex. Fluorescence quantum yield (ϕ_F), fluorescence decay times (τ_F) and radiative (k_R) and nonradiative (k_{NR}) rate constants (k_{NR}) are given [83]

dark state (n, π*), leading to fast non-radiative decay. Since the (n, π*) state is lower in energy than (π, π*), it results in weak fluorescence and short lifetime value [83]. This shows that, even in molecules where the AIE effect is potentially present, the balance between the increase or decrease of photoluminescence may also depend on the nature of the two lowest lying singlet excited states, and not only due to a restriction of the molecular motion process.

3 Photophysical Studies of AIE-Luminogens

3.1 TPE Derivatives

A good–bad solvent mixture constitutes a consensual strategy to study AIE behavior in dilute solutions of potential AIEgens [91]. Since TPE derivatives are typically aromatic-like (hydrophobic) molecules, water is a poor solvent, and is therefore used as the most common bad solvent in combination with water-miscible good solvents such as THF, acetonitrile, dimethylsulfoxide and 1,4-dioxane. Formation of nanoaggregates in suspension, in solvent–nonsolvent mixtures, may also lead to the Mie scattering effect [92], detected by the appearance of a long wavelength tail in the absorption spectrum [93].

TPE is, as described, one of the most flowing sources of AIEgens. This is in part due to its structural modification (rigidification) in the excited state, but also to the development of simplified strategies of synthesis and derivatization of this molecule [43]. Scheme 4 depicts some illustrative **TPE** derivatives synthesized by several research groups [94–98].

Increases in the photoluminescence efficiency in the solid state, or from a bad-solvent to a good-solvent fraction, may be significantly different depending on the system; this happens even among several TPE derivatives (Table 1). The AIE factor (α_{AIE}), defined as the ratio between the ϕ_F values of the aggregate and of the monomer (isolated molecule in a good solvent), constitutes a parameter that establishes a qualitative manner of measuring the emission increase due to the AIE. Table 1 summarizes some of the relevant literature data on TPE derivatives with data obtained from photophysical studies [94–98]. As noticed in Table 1, the value of α_{AIE} is structure dependent, and so is the dominant intramolecular motion, restricted when aggregation occurs, acting as an active dissipation factor for the radiationless deactivation [99]. In Table 1 and Scheme 4, it is worth noting the highest α_{AIE} values for compounds **15** and **16**, which are ca. 9.5 times higher than those of TPE.

AIEgens oligomers generally possess twisted conformational structures in the ground state, and hence afford a more moderate packing pattern than traditional luminogens with a planar structure. This facilitates the interplay between different morphologies by heating, solvent fuming, mechanical stimuli such as pressing, grinding and so forth, in particular upon structural change promoted by light excitation [100]. Emission of many AIEgens can be switched through modulating morphology of the luminogen between amorphous and crystalline states [101]. Consequently, several AIEgens present mechanoluminescence (ML) properties [26, 101–106], which have been the subject of extensive reviews in the past 5 years

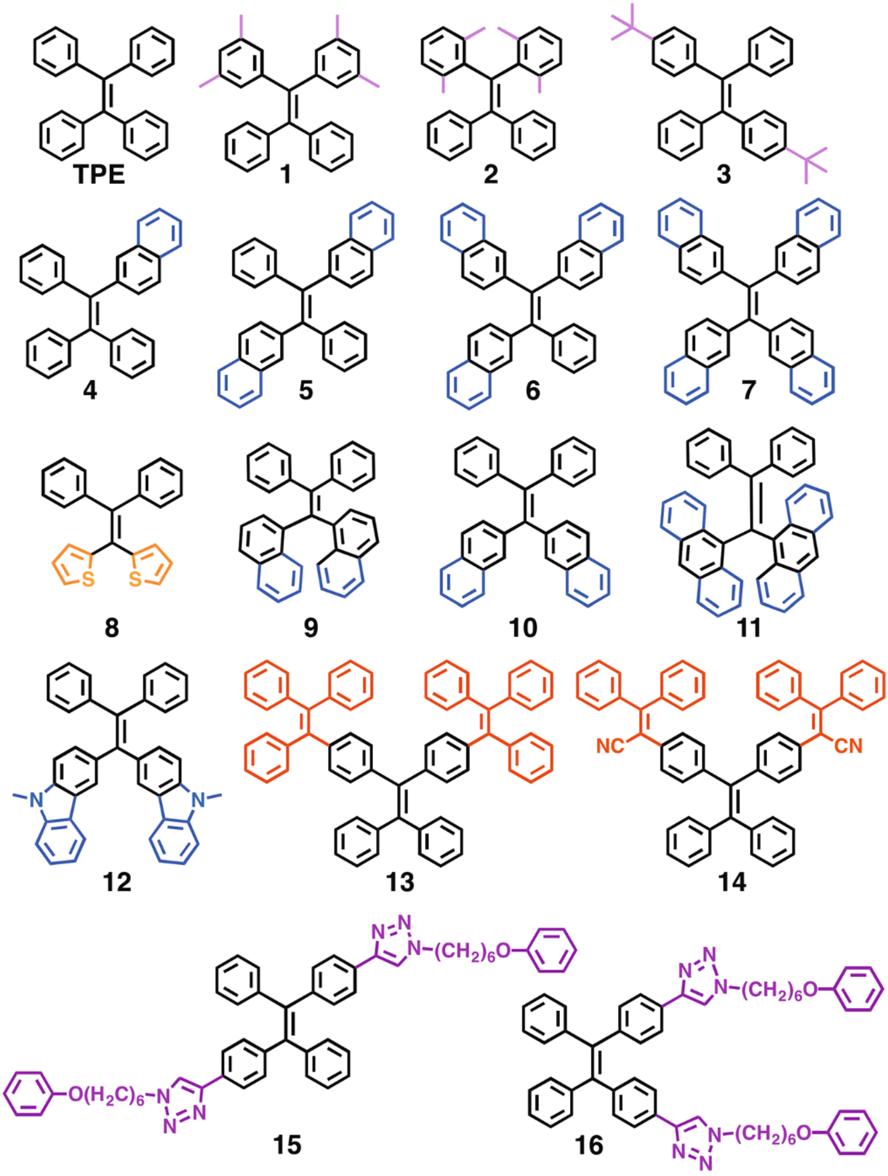

Scheme 4 Comparison of TPE and some TPE derivative structures described in the literature. The core structure of TPE is highlighted in black and red (for compound **13**)

[100, 107–110]. Among those AIE-active and ML responsive compounds, TPE [108, 111], distyrylanthracene (DSA) [110], diphenylbenzonfulvene (DPBF) [26, 101, 106] and phenothiazine (PTZ) [112–116] derivatives are likely to be within the more extensively investigated (Scheme 3).

Table 1 Comparison of fluorescence quantum yields for tetraphenylethylene (TPE) derivatives in solution, mixture of good solvent/bad solvent and in solid state, both powder and film, where data are available, along with the aggregation-induced emission (AIE) factor (α_{AIE}), which discriminates the enhancement of the fluorescence upon aggregation

Compound	Solution	Good solvent/ bad solvent	Powder	Film	α_{AIE}[a]
TPE	0.003	0.25	0.23	0.26	87
1	0.006	0.075	0.30	n.a.[b]	50
2	0.60	0.75	0.98	n.a	1.6
3	0.024	0.20	0.14	0.46	19
4	0.003	n.a	n.a	0.45	56
5	0.003	0.043	0.14	0.12	47
6	0.016	n.a	n.a	0.37	23
7	0.017	n.a	n.a	0.22	13
8	0.002	0.007	n.a	n.a	3.3
9	0.017	0.13	n.a	n.a	7.3
10	0.004	0.04	n.a	n.a	10
11	0.097	0.18	n.a	n.a	1.9
12	0.004	0.13	n.a	n.a	33
13	0.004	0.46	n.a	n.a	115
14	0.003	0.13	n.a	n.a	43
15	0.001	0.39	1.0	n.a	833
16	0.001	0.40	1.0	n.a	833

Compound numbers are related to structures in Scheme 4. Data obtained from [94–98]

[a] $\alpha_{AIE} = \Phi_F^{agg}/\Phi_F^{sol}$, where ϕ_F^{agg} = highest fluorescence quantum yield of the aggregate form and ϕ_F^{sol} = fluorescence quantum yield diluted in solution

[b] Data not available

3.2 Phenothiazine Derivatives

PTZ is a well-known heterocyclic compound [117], with a twisted butterfly-like structure, with electron-rich nitrogen and sulfur heteroatoms, and therefore with a strong electron donor character. This favors the presence of a lowest lying n,π^* singlet excited state and favors intersystem crossing between the excited singlet and triplet states (with different state configurations) according to El-Sayed rules [118], opening a potential new emissive channel and class of molecules: PTZ-based luminogens with thermally activated delayed fluorescence (TADF) [119, 120]. Due to its non-planar bending “butterfly” shaped conformation [121], PTZ’s ring may avoid intermolecular interactions, such as π–π stacking, which are typically responsible for ACQ. This has led to the use of the PTZ group as a basic chromophoric structure platform for the design of new AIE luminogens [122, 123].

Tang et al. [124] prepared a series of phenothiazine-based red/near infrared (NIR) fluorophores, found AIE-active, using 10-butyl-phenothiazine-3-carboxaldehyde as starting material. Among them, PTZ1 and PTZ6 presented higher ϕ_F, of 0.234 and 0.207, respectively, with $\lambda^{em} > 610$ nm in the solid state (Fig. 3). In these PTZ compounds, the mechanism of the AIE behavior was further explored

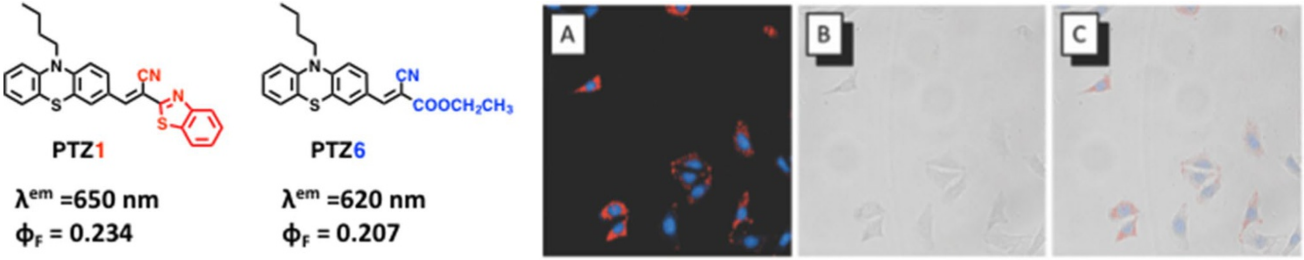

Fig. 3 Left panel Chemical structures of PTZ1 and PTZ6 along with their respective emission maxima and fluorescence quantum yield in solid state. Images on the right display confocal microscopy images of HeLa cells stained with PTZ6: **a** fluorescence, **b** bright-field and **c** merged (nuclei stained by commercially available nuclei imaging agent Hoechst 33342). Adapted from reference [124], with permission from RSC, Copyright 2019

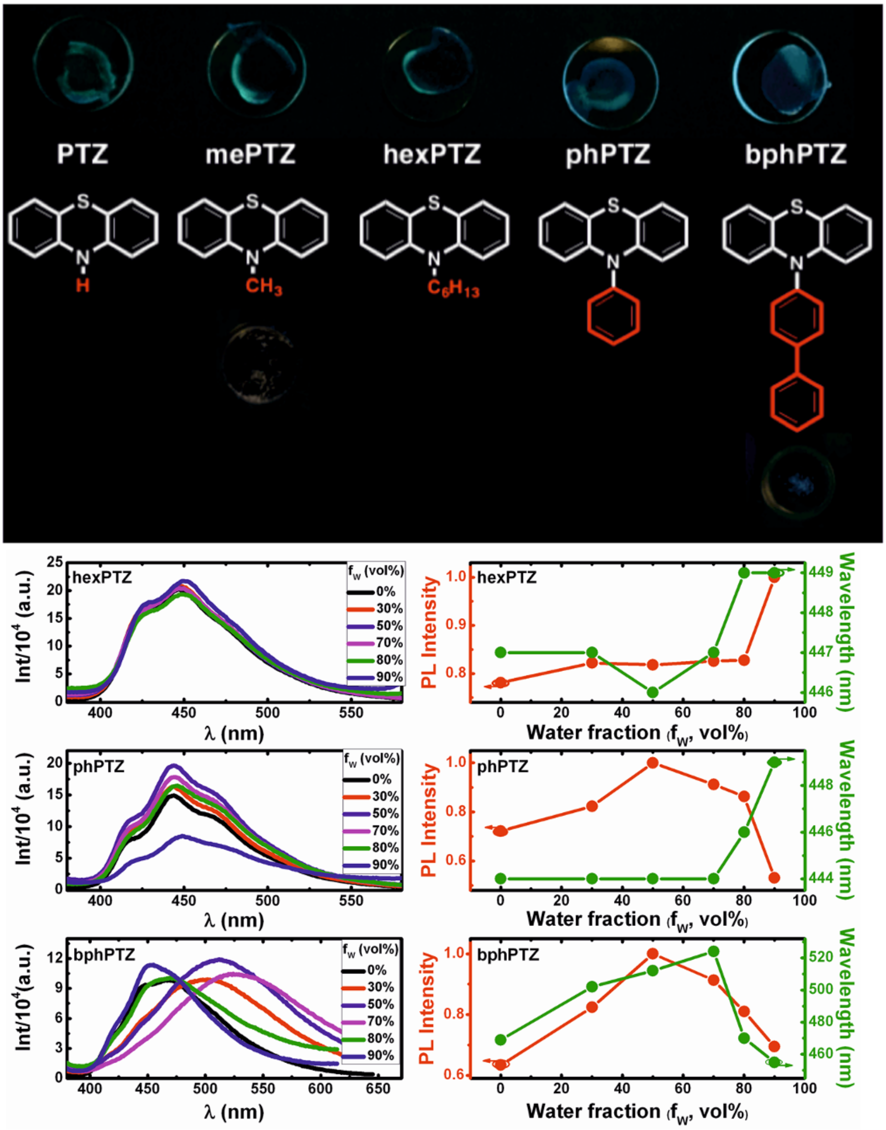

Fig. 4 Photophysical studies of *N*-alkyl and *N*-aryl substituted phenothiazines (PTZs). Structures, acronyms and solid state emission (top images thin films, bottom images powder) under UV-illumination. Fluorescence emission spectra for the *N*-substituted PTZs in THF:water mixtures and their respective correlation of photoluminescence intensity and fluorescence emission maxima (λ^{em}) with the mixture water fraction (f_W = 0–90%). Adapted from reference [125], with permission from Elsevier, Copyright 2020

[124]. Single-crystal analysis of PTZ1 suggested that the butterfly-shaped geometry was partially responsible for the higher emission efficiency in solid or aggregated states than in solution, with the *n*-butyl group acting as a spacer to

separate neighboring molecules. The high ϕ_F and red/NIR emission made those dyes favorable for biological imaging, with PTZ6 being used to stain HeLa cells. Indeed, PTZ6 was found to accumulate mainly in lipid droplets (LDs), with better a performance when compared to traditional LD tracking agents such as Nile red. This selectively of PTZ6 was suggest to result from the hydrophobic *n*-butyl group.

The design of new PTZ derivatives with AIE properties require a deeper understanding of the photophysical properties and photostability of this class of compounds. A comprehensive study of the photophysical properties of five *N*-alkyl and *N*-aryl substituted PTZs was reported recently (Fig. 4) [125].

The electronic spectral properties (of both singlet and triplet states) and fluorescence quantum yields (ϕ_F) in solution were found to be poorly affected by substitution. The *N*-methyl and *N*-phenyl substituted phenothiazines, mePTZ and phPTZ, respectively, showed higher ϕ_F values in the solid state, either in thin films or powder, than in solution. It was found that the solid state (powders) of mePTZ and bphPTZ derivatives exhibit room temperature phosphorescence (RTP, Fig. 4). Moreover, and more interestingly, the photostability and AIE properties were found to be dependent on the *N*-substituent (alkyl versus aryl). In polar solvents, PTZ and mePTZ were found to undergo self-sensitized photooxidation upon UV-irradiation while the *N*-aryl substituted phenothiazine, bphPTZ, was found to be photostable. Nonetheless, for the *N*-alkyl derivative, hexPTZ, an increase in total emission, together with a red-shift of emission maxima, was found for the mixture with the highest water fraction content, $f_W > 80\%$, thus showing AIE. A different behavior was observed for the *N*-aryl derivatives, phPTZ and bphPTZ, where, after a first increase in total emission up to the fraction mixture $f_W = 50\%$, ACQ is observed thereafter, which, also based on TDDFT calculations, was attributed to the adoption of a different conformation for phPTZ and bphPTZ, which was also found to be water (in THF: water mixtures) content dependent.

3.3 Distyrylanthracene Derivatives

Distyrylanthracene (DSA), divinylanthacenes (DVA), distyrylbenzene (DSB) and derivatives, have also been reported as stimuli responsive smart materials [126] with high solid-state emission [127]. Tian et al. [128] provided some photophysical insights on the origin of the AIE phenomenon in a series of DSA derivatives (Fig. 5), using steady-state and time-resolved fluorescence.

In dilute solutions, DSA derivatives display a twisted structure in the ground state that, upon excitation, ultimately relaxes, within several picoseconds, to a planar structure [128]. With the DSA derivatives, a more extended conjugation is observed in the excited state (electron cloud more delocalized) leading to a more stabilized and rigid structure. Comparing the derivatives, those with electron-donating groups (BMOSA and BTVA) have higher radiationless rate constant values, k_{NR}, whereas the DSA-derivative with electron-withdrawing group (BP2VA) display the smallest k_{NR}. In good solvent solutions, the radiationless decay channel dominates the

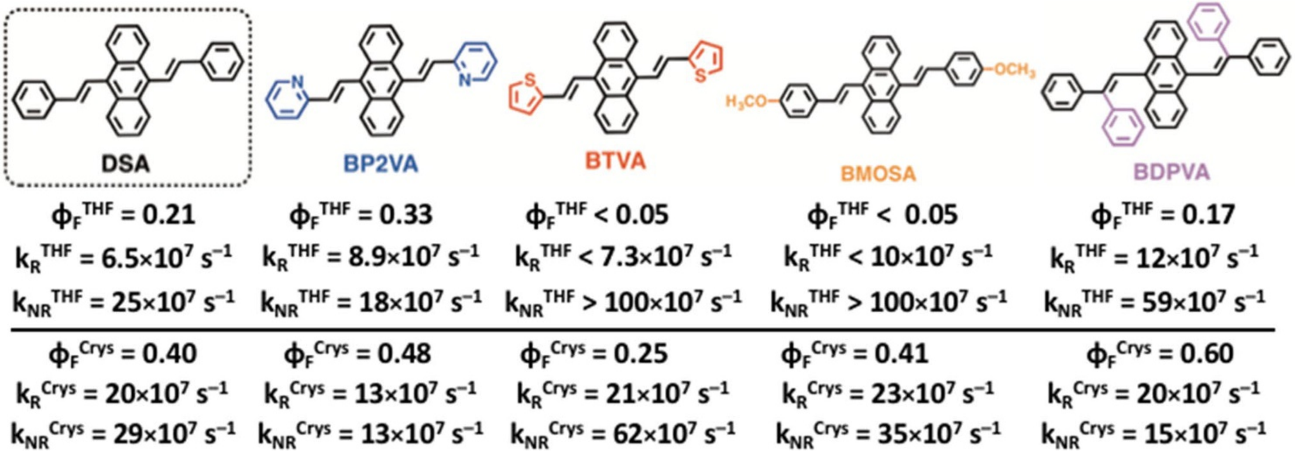

Fig. 5 Structures and acronyms of distyrylanthracene (DSA) derivatives, along with their respective fluorescence quantum yields (ϕ_F) and rate constants in THF and crystal (Crys) [128]

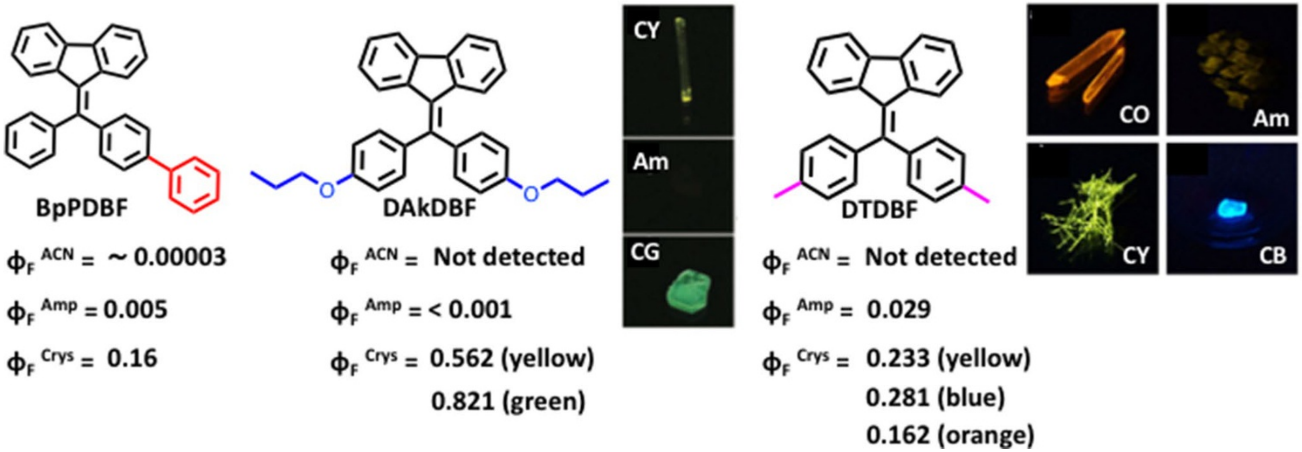

Fig. 6 Structures and respective fluorescence quantum yields (ϕ_F) of diphenylbenzonfulvene (DPBF) derivatives BpPDBF, DAkBDF and DTDBF solids. Photos of DAkBDF and DTDBF solids under UV illumination: *Am* amorphous powder, *CY* yellow crystal, *CG* green crystal, *CO* orange crystal, *CB* blue crystal. Adapted from Refs. [101] and [106], with permission from Wiley, Copyright 2020

deactivation of the excited state (k_{NR} is at least three times higher than k_R) of DSA and derivatives. In contrast, the nonradiative deactivation is greatly suppressed by molecular stacking in the aggregates, here studied either in single crystal structures or supported in polymethylmethacrylate (PMMA) films, and consequently the fluorescence is significantly enhanced (e.g., for BMOSA, ϕ_F in crystal is over eight times higher than in THF solution).

4 AIE and CIE in Small Molecules

Diphenylbenzonfulvene (DPBF) derivatives are known to display another AIE-related property: crystallization-induced emission (CIE). DPBF derivatives are almost non-emissive in solution and amorphous state, but highly emissive in the crystalline state [111]. BpPDBF (Fig. 6) crystals emit an intense blue light upon UV-excitation, while its amorphous powders emit a faint yellow light; in the good solvent acetonitrile, BpPDBF is poorly emissive [26]. Notably, the ϕ_F of BpPDBF crystal is 32 times higher than that of its amorphous powder. The CIE effect is noticed even more dramatically for DAkBDF (Fig. 6); indeed, while its amorphous powder is practically non-emissive (<0.001), in its crystal structures it shows high ϕ_F values (0.56–0.82) [106].

Dong et al. [101] replaced alkoxy phenyl groups with tolyl groups with ditolyldibenzofulvene (DTDBF, Fig. 6) leading to a twisted conformation, bulky conjugation core and peripheral tolyl groups. As described with DPBF [24] and other derivatives [25, 129], DTDBF preserved the AIE-active core: while it is nearly non-emissive in pure acetonitrile, its emission intensity was gradually augmented upon gradual addition of water in acetonitrile:water mixtures. For DTDBF, more interesting was to observe three single crystals of this compound with varied emission colors (Fig. 6). The molecular conformations, packing patterns and interactions in the three crystal structures of DTDBF were investigated. Specific strong intermolecular interactions (such as π–π stacking or H-/J-aggregates) were

Table 2 Comparison of the optical and photophysical properties of ditolyldibenzofulvene (DTDBF) solids in crystalline and amorphous states [101]. See sample structures in Fig. 6

Sample	λ^{em} (nm)[a]	ϕ_F[b]	A1/A2[c]	τ_1 (ns)	τ_2 (ns)	$k_F \times 10^{-7}$ (s^{-1})[d]	$k_{NR} \times 10^{-8}$ (s^{-1})[e]
CO	586	0.162	100/0	1.7		9.53	4.99
CY	545	0.233	100/0	2.9		8.03	2.64
CB	461	0.281	100/0	39.2		0.72	0.18
Am	557	0.029	80/20	0.9	1.9	2.64[f]	8.83[f]

[a] Emission maximum

[b] Fluorescence quantum yield determined with an integrating sphere with $\lambda^{ex} = 340$ nm

[c] Fraction (A, %) and lifetime (τ, ns) of shorter (1) or longer lived species (2)

[d] $k_F = \frac{\phi_F}{\tau_F}$;

[e] $k_{NR} = \frac{(1-\phi_F)}{\tau_F}$;

[f] Determined with an average lifetime, $<\tau> = 1.1$ ns

ruled out due to the twisted molecular conformations in all the crystal structures of DTDBF. Thus, the emissions of those crystals should occur from a single molecule which depends mainly on its molecular conformation. The asymmetric units of CB, CY and CO contain one, three, and six molecules of DTDBF respectively. The more C–H···π interactions presented in the crystal structure, the higher the photoluminescence efficiency (Table 2). The existence of these weak interactions between molecules helps lock the motion of the aryl rings, and, hence, to rigidify the molecular conformation [100], with consequent increase in photoluminescence efficiency due to CIE. While the three crystal structures display single exponential fluorescence decays, the amorphous solid of DTDBF displays a bi-exponential decay, with 80% contribution of the short-lived component and 20% of the long-lived component, suggesting the availability of fast decay processes due to the loose packing pattern (Table 2). The lifetime increases promptly with the number of C–H···π interactions when comparing the three crystal structures, which also agrees with the increase in photoluminescence efficiency. Nonetheless, the fluorescence quantum yield in crystalline form is at least five times higher than in amorphous powder.

Another luminogen core molecule that matches both ML properties with high emission efficiency in the solid state (CIE) is triphenylacrylonitrile (TPAN), see structure in Fig. 7 [111]. Combination of TPAN with diaryl [130] and tryphenylamine [131, 132] groups introduces donor–acceptor (D–A) characteristics into these systems, making these AIE-active luminogens into molecules with intramolecular charge transfer (ICT) character and ϕ_F values close to 1.0 in solid powder. The TPAN moiety was also attached to the backbone of electron-rich *N*-heterocycles to design D–A polymers that feature AIE properties (see next section) [133–136].

5 Design and Photophysical Studies of AIE-Active Polymers

Until 2 years ago the literature regarding the AIE effect in polymers was relatively limited, particularly when compared with oligomers showing this effect. This has generated increased interest, which led to a growth in publications of AIE effect in polymers from ~ 100 papers in 2016 to 190 in 2019. Although less attention has been devoted to polymers with AIE, several reviews have been published concerning synthetic strategies and smart material applications [56, 57, 137, 138] of AIE polymers, their mechanochromic fluorescent properties [139] and some specific applications of these polymers in biological systems [140] and as detector sensors for explosives [141].

5.1 Building AIE-Active Polymers from Small Molecules with AIE Properties

AIE-active polymers built from a combination of polycarbazoles and polytriphenylamines backbones (donor) and TPAN (acceptor) moieties were studied for the detection of 1,3,5-trinitrobenzene (TNB), used as prototypical nitroaromatic explosive, in THF:water mixtures [133]. Detection of TNB by fluorescence spectroscopy

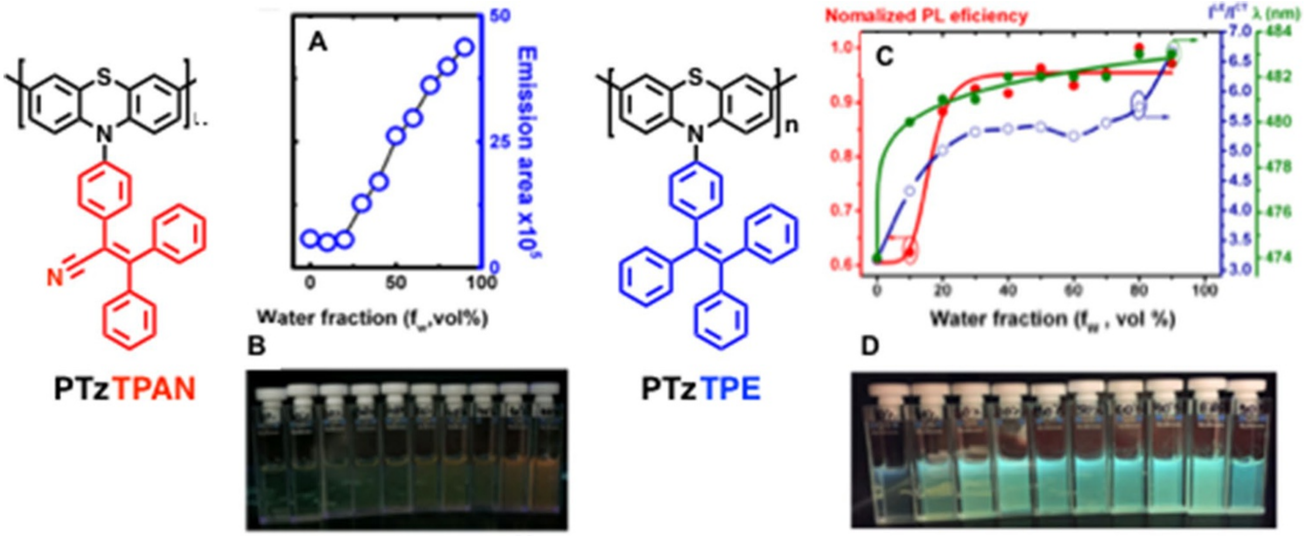

Fig. 7 Photophysical studies of PTZ-based polymers. PTZ-triphenylacrylonitrile (PTzTPAN): **a** Correlation of emission area with increasing water fraction in THF:water mixtures and **b** photos under UV irradiation (with $\lambda^{ex} = 365$ nm) of PTzTPAN in THF:water mixtures (from left 0% to right 90% with increments of water fraction (v/v) of 10%). PTZ-tetraphenylethene (PTzTPE): **c** correlation of emission area, maximum emission wavelength and ratio of intensity of locally excited (LE) versus charge transfer (CT) emission band with increasing water fraction for in THF:water mixtures for PTzTPE. **d** Photos under UV irradiation green fluorescence emission of PTzTPE in THF:water mixtures (from left 0% to right 90% with increments of water fraction (v/v) of 10%). Adapted from reference [142] with permission from ACS, Copyright 2018

at low polymer concentrations by the quenching of the emission of the polymers upon addition of TNB was investigated. The quenching mechanism was found to be based on electron transfer between the excited state of the polymers and the nitroaromatic analyte [133, 141].

The TPAN structure was also used for the construction of another AIE-active polymer, PTzTPAN (Fig. 7) [142]. With this polymer, the electron-rich backbone used was from another AIE building block: phenothiazine (PTz acronym in the polymer). This PTz-based polymer PTzTPAN, together with PTzTPE, a polymer based on the PTz backbone and the TPE moiety (Fig. 7), were further investigated as AIE luminogens [142].

PTzTPAN displays a significant red-shift (~100 nm) in the photoluminescence spectra on going from THF solution to the solid state, and the polymer was found to be non-emissive in polar solvents, such as DMF, and poorly emissive in non-polar solvents ($\phi_F = 0.006$ in dioxane and 0.002 in THF) and in the solid (powder) with $\phi_F = 0.002$ [142]. In classical good:bad solvent mixtures, THF:water, a clear enhancement of fluorescence emission was observed for mixtures with water fraction (f_w) ≥ 40%, also followed by a red-shift of the emission [142]. The red-shift was attributed to the behavior of charge transfer (CT)-type bands with an increase in solvent polarity, in this case through an increase of the water fraction. In the good:bad solvent mixtures, ϕ_F was found to increase five times: 0.002 in THF to 0.010 in $f_w = 90\%$ [142]. With PTzTPE, the increase in the water amount in THF: water mixtures led to a gradual increase of ϕ_F up to $f_w = 40\%$. Nonetheless, for PTzTPE, a decrease in CT band intensity upon the addition of water was observed [142]. Very interestingly, this showed that, for PTzTPE, concomitant with the gradual increase in the AIE effect, a decrease in CT contribution is observed, thus showing that the latter is in competition with the AIE process. Even more fascinating than the competition between the CT and AIE effects was the fact that, in dioxane:water mixtures, PTzTPE showed ACQ with the gradual increase of water (from $\phi_F = 0.14$ in pure dioxane to 0.042 in $f_w = 90\%$). Indeed, selective AIE behaviour in specific solvents was previously reported for D–A systems; the main cause for this was attributed to the transition from the emissive locally excited (LE) state to the dark CT state [72, 143]. Furthermore, time-resolved fluorescence measurements were performed to characterize the coexistence of these states in PTzTPE solution and powder (Fig. 8). In general, the shortest and the longest decay times are associated with the emission of the LE and CT species (τ_1 and τ_3) with decay times varying from 51 to 103 ps (LE) and 4.7 to 5.6 ns (CT), which can be seen by the pre-exponential factors, a_{i1}, when the decays are collected at 500 nm (in the LE state emission band) and a_{i3} for $\lambda^{em} > 600$ nm (CT band). One of the most interesting features of these decays is the presence of the intermediate decay component (τ_2) in the solid state (powder), dioxane, and in the solvent mixtures with water; in THF, this intermediate lifetime, τ_2, is found to be absent (Fig. 8). In dioxane:water and THF:water mixtures, the pre-exponential values associated with this middle decay time (τ_2) component increase concomitantly with the increase in the water fraction. The τ_2 decay component could therefore be assigned to the emission of the polymer emissive aggregate, which was found to be present even in dioxane. Furthermore, fs-transient absorption (fs-TA) data obtained in THF shed light on the observed behavior, showing that aggregation

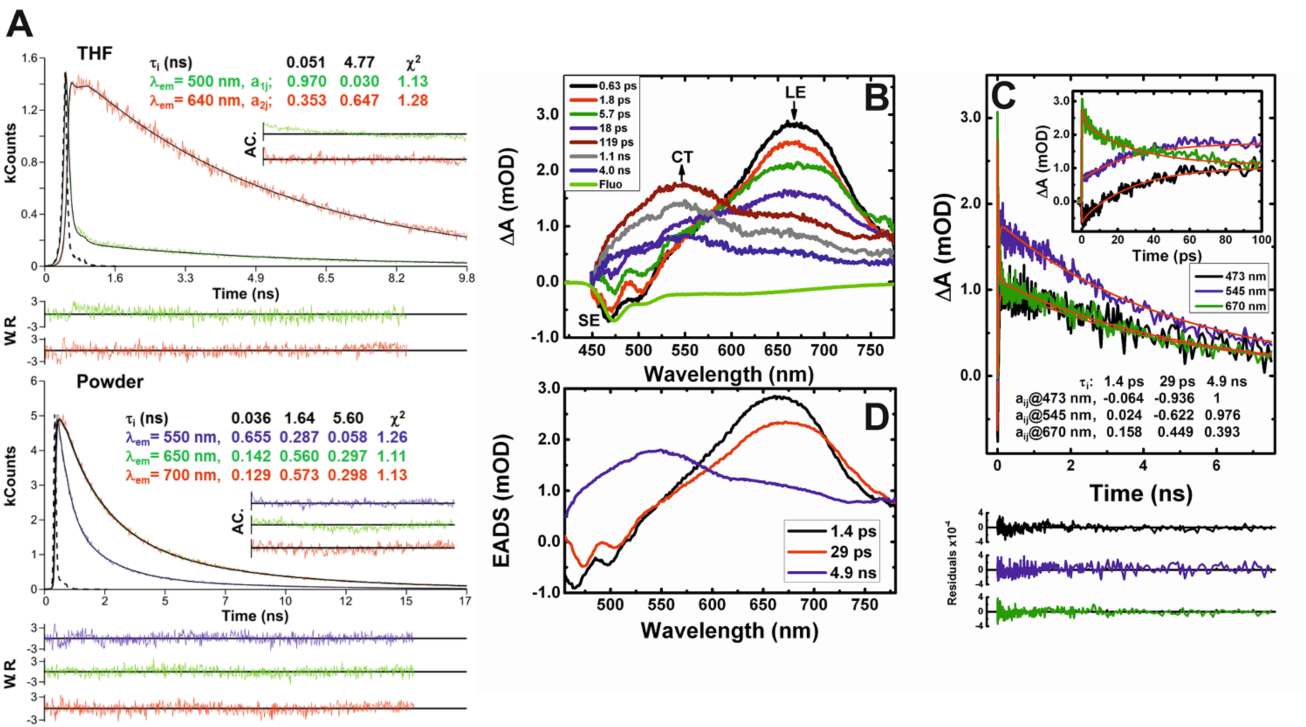

Fig. 8 **a** Room temperature fluorescence decays for PTzTPE collected with excitation at 404 and 451 nm in THF solution and in the solid state (powder), respectively. **b** Room temperature femtosecond time-resolved transient absorption (fs-TA) data for PTzTPE in THF solution collected with excitation at 430 nm. **c** Representative kinetic traces. **d** Evolution-associated difference spectra (EADS) obtained from global analysis of the TA data. *Insets* in **c** are the decays at shorter times. Adapted from reference [142] with permission from ACS, Copyright 2018

of the PTzTPE polymer indeed does not occur in THF. The fs-TA studies also showed that the CT state was formed both from direct excitation in the ground-state or at the expense of the decay of the LE excited state.

As shown in the previous examples, the general strategy for the preparation of AIE polymers involves incorporation of AIEgens, such as HPS, TPE [136], TPAN and DSA [140], into the backbone structure or grafted onto the polymer skeleton with different synthetic and polymerization strategies [56, 57].

5.2 TPE-Based Conjugated Polymers

TPE-based conjugated polymers—poly(arylene-diphenyl-vinylenes)—have been known since the 1960s [144]. Some of them show distinct AIE properties leading to high solid-state photoluminescence quantum yields—higher than 70% for some poly-TPEs [145]. The easily functionalized four phenyl rings of the TPE unit were combined with a variety of reactive groups in the synthesis of TPE-based polymers with inherent porosity [146]. The development of microporous organic polymers (MOPs) with very high surface area is an active field of current research [147], with high potential in a variety of applications [145, 148, 149], such as energy storage, light harvesting, catalysis and sensing of hazardous chemicals and explosives. A recent study on the photophysical properties of two types of poly(1,4-phenylene-diarylvinylene)s with 4-tert-butylphenyl (Poly-t-Bu in Fig. 9) or naphthyl (Poly-Np1 and Poly-Np2 in Fig. 9) as aryl substituents at the vinylene units as well as the corresponding poly(1,3-phenylene-dinaphthylvinylene), either in solution or in the solid state (powder and films), was made to evaluate the effect of aggregation on the photoluminescence efficiency, but also the polymer porosity [98].

When AIEgens, such as TPE and derivatives, are chemically incorporated into polymeric structures, they may import their AIE properties [138, 150, 151]. With this in mind, it was anticipated that the polymers Poly-t-Bu, Poly-Np1 and Poly-Np2, whose monomeric model compounds are AIE active, would also maintain their AIE properties. Although Poly-t-Bu showed an increase of fluorescence quantum yield upon the increase of the water fraction, the fluorescence of the naphthyl polymers is quenched with the addition of bad-solvent water in THF:water mixtures. Actually, as shown in Fig. 9, Poly-Np1 and Poly-Np2 presented ACQ. Moreover, the ϕ_F of Poly-Np2 is smaller than Poly-Np1 either in solution (when compared at the same f_W in THF:water mixtures) or in solid state [98]. The ACQ behaviour of naphthyl polymers may be caused by the π-stacking tendency of the naphthyl groups, leading to the formation of H-type aggregates. However, Poly-t-Bu presented a high photoluminescence quantum yield in solid state with $\phi_F = 0.64$ in film—an increase of ca. 14 times when compared to THF. Moreover, in $f_W = 90\%$, an almost equal value is obtained, $\phi_F = 0.62$ [98]. This high ϕ_F was found accompanied by distinct microporosity in the solid state with a high Brunauer–Emmett–Teller (BET) surface area, S_{BET}, value of 417 $m^2\ g^{-1}$, probably driven by the steric demand of the tert-butyl groups. Conversely, the occurrence of π–π interactions may also lead to tight packing of Poly-Np1 and Poly-Np2, since these polymers do not show intrinsic microporosity ($S_{BET} < 17\ m^2\ g^{-1}$) [98].

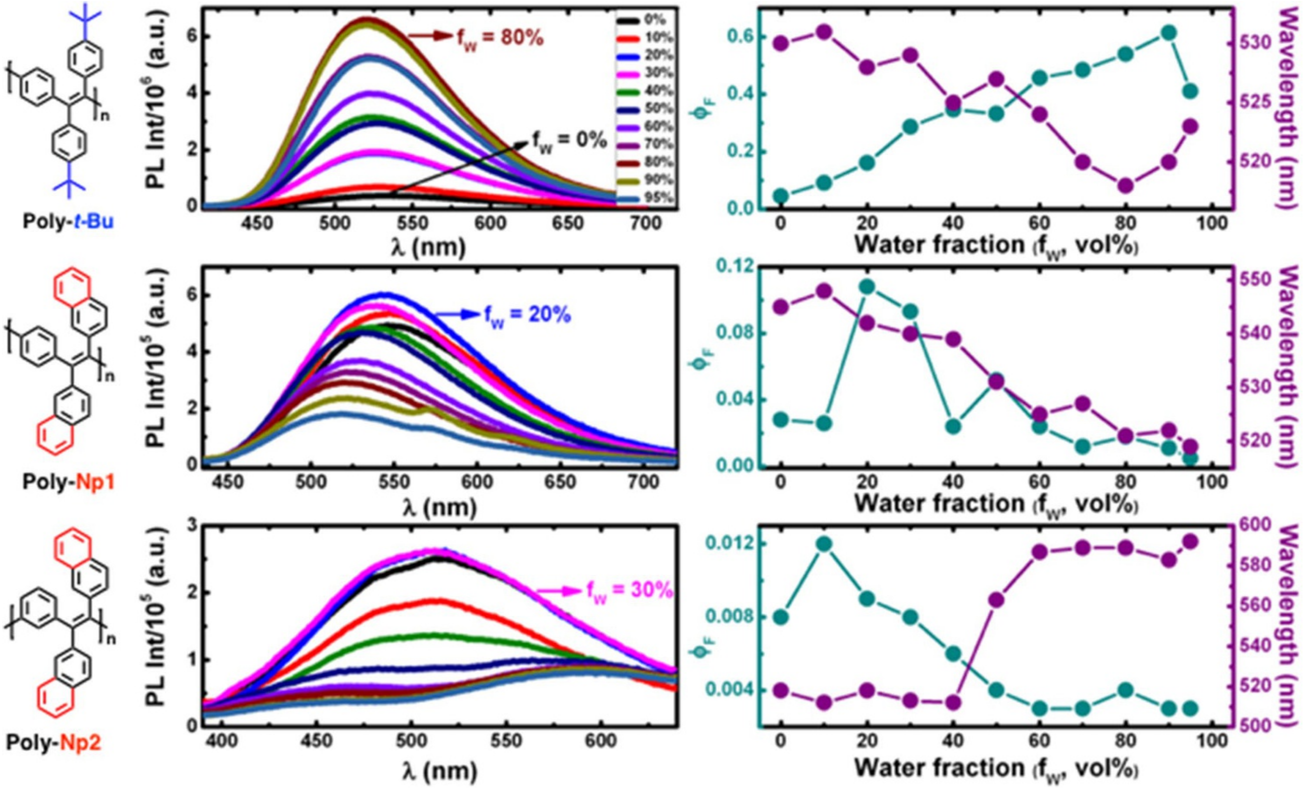

Fig. 9 Room temperature fluorescence emission [photoluminescence (PL)] spectra of the polymers Poly-t-Bu, Poly-Np1 and Poly-Np2 in THF:water mixtures and their respective correlation of the fluorescence quantum yield and emission maxima with increasing water fraction, $f_W = 0–95\%$. Adapted from reference [98] with permission from RSC, Copyright 2020

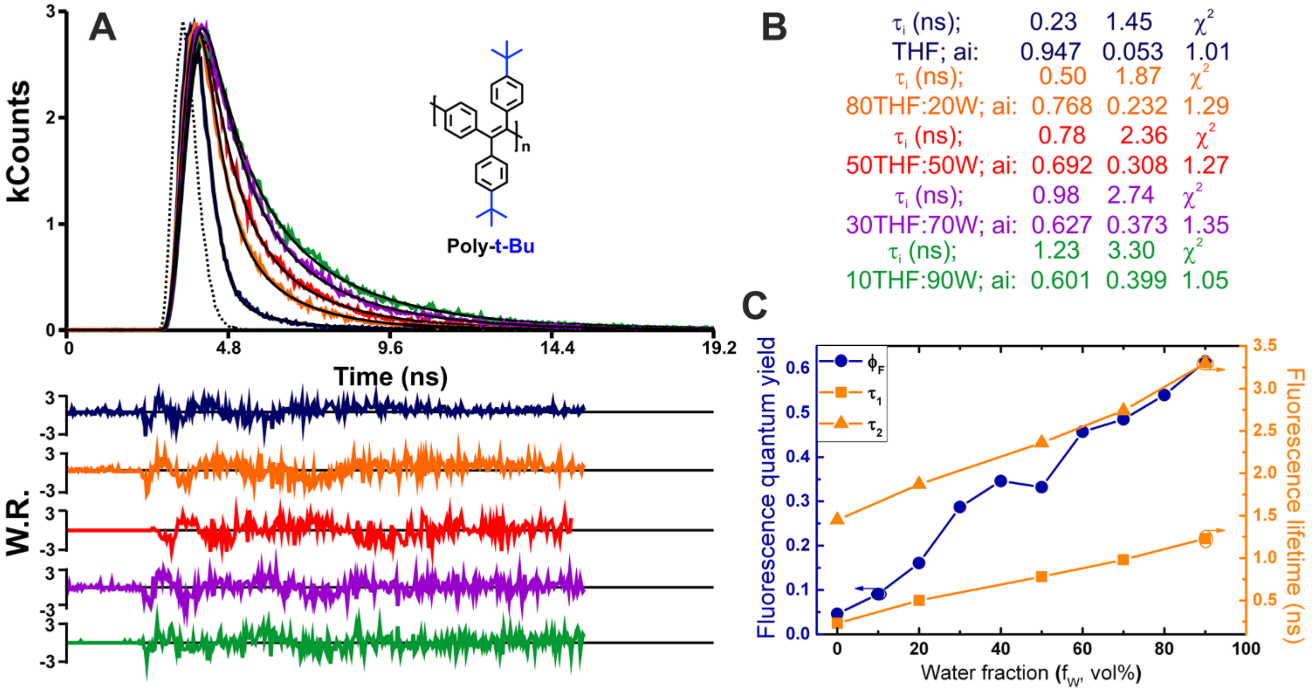

Fig. 10 **a** Room temperature fluorescence decays for Poly-t-Bu collected in THF solution and in THF:water mixtures. **b** Fluorescence decay times and χ^2 values of the analyzed decays of Poly-t-Bu in the different THF:water mixture. **c** Correlation of fluorescence quantum yields and fluorescence decay times for Poly-t-Bu with increasing water fraction (f_W) in THF:water mixtures. Adapted from reference [98] with permission from RSC, Copyright 2020

Time-resolved fluorescence decays were also obtained in order to gain further insight into the precise nature of the AIE phenomenon in Poly-t-Bu. The fluorescence decays of Poly-t-Bu in THF and THF:water mixtures were found to be well fitted with a bi-exponential decay law, thus indicating the presence of two emitting species in the aggregate region ($\lambda^{em} = 525$ nm) [98]. This possibly indicates that the emissive aggregate results from two main conformers with different contributions to the photoluminescence decay. For Poly-t-Bu in THF, a fast decay component, τ_1, in the 0.23–1.2 ns range together with a longer decay time component, τ_2, varying from 1.5 to 3.3 ns, were found on going from 0 to 90% water content in THF:water mixtures [98].

As seen in Fig. 10, the fluorescence quantum yields and the fluorescence lifetimes of Poly-t-Bu follow a similar trend, i.e., a concomitant increase of these parameters with the increase in water content. In addition, the determination of the radiative (k_F) and radiationless (k_{NR}) rate constants (avoiding average lifetime contributions and instead considering the longer decay time, τ_2, usually associated to a higher fractional contribution, C_i, to the decays) clearly showed a decrease of k_{NR} and an increase of k_F with f_w. The radiationless decay is therefore dominant up to $f_w = 70\%$, and, from there onwards, the radiative deactivation begins to dominate, mirroring a high contribution of this deactivation channel due to the AIE effect [98].

Conjugated polymers (CPs) have great potential in various applications ranging from electronics, aerospace, sensing, catalysis and energy; hence there is intensive investigation of these materials [152]. Their electronic properties are, however, highly dependent on the physical conformation of the polymeric chains and the way these chains pack together in films [153]. An obstacle to their development is the significant fluorescence quenching in the solid state that generally occurs due to strong interchain interaction, as in the example of the polythiophenes [154]. On the other hand, oligo- and poly-thiophenes embrace one of the characteristics associated with the AIE effect: structural rigidification in the excited state. Whereas in molecules where this AIE effect occurs, the generic mechanism involves rigidification associated to close proximity of another molecule (aggregation-induced), in oligo- and poly-thiophenes this essentially results from the quinoidal-like structure (extended π-conjugation), in contrast with the possibility of a more twisted conformer(s) (and this depends on the substitution) in the ground state [155–158]. This obviously paves the way for the study of oligo-and poly-thiophenes as potential AIEgens.

To try to overcome the ACQ effect, two TPE-polythiophenes, homoPT and coPT (structures in Fig. 11), with different degrees of TPE substitution were recently investigated [153]. The introduction of the propeller-shaped TPE units prevent the molecules from packing in a π–π stacking process in the polymeric aggregate, therefore precluding emission quenching of these polythiophenes in the solid state. To understand the role of the sterically bulky TPE pendant groups on the inhibition of intra- and/or interchain packing (aggregation) of these conjugated polymers, photohysical studies were performed with poly(3-hexylthiophene), P3HT, with similar average molecular weight, used as a "pure" model polythiophene, and a TPE-thiophene (T-TPE) model oligomeric compound. Unlike what was predicted (TPE

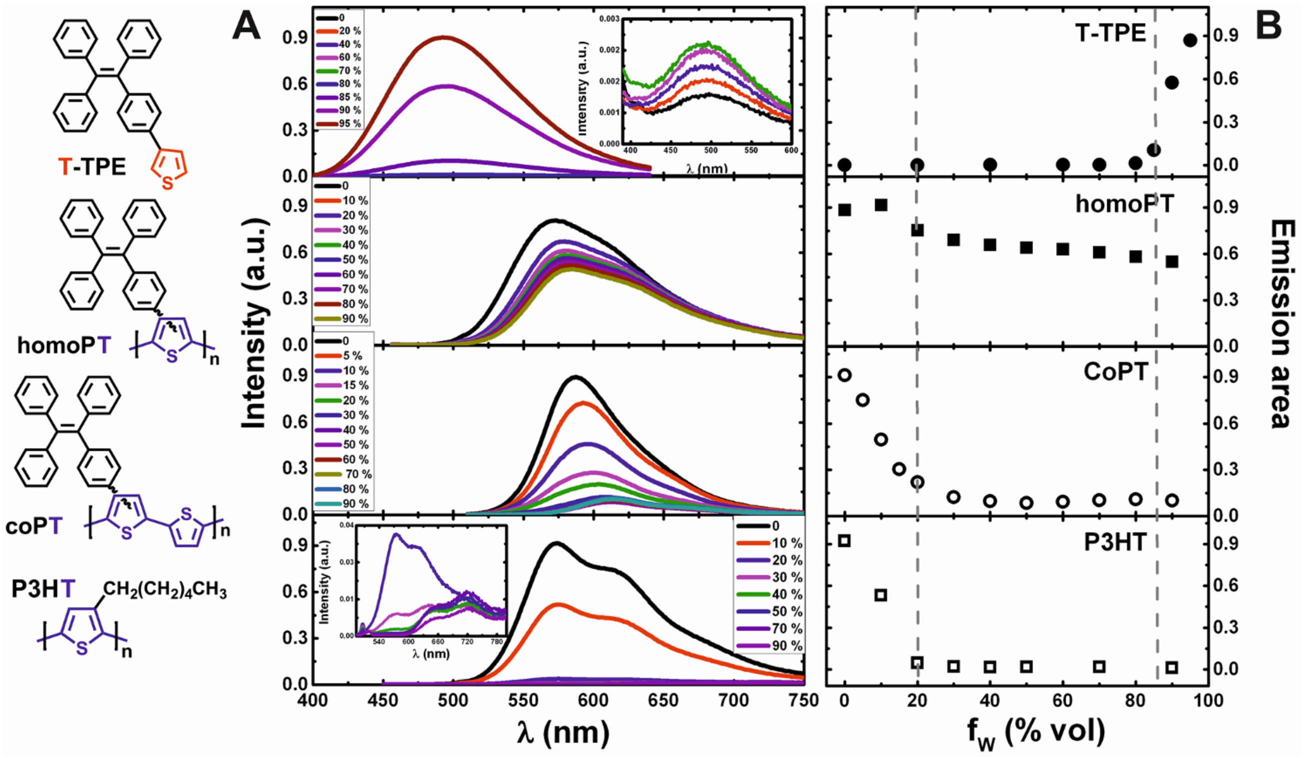

Fig. 11 Structures and acronyms of model compound and poly-thiophenes. **a** Fluorescence emission spectra and **b** correlation of emission area with increasing water fractions (f_w) in THF/water mixtures for the polythiophenes, homoPT, coPT, and P3HT, together with the model compound T-TPE. Adapted from reference [153], with permission from ACS, Copyright 2020

preventing π–π stacking and consequent quenching of emission), homoPT and coPT, as well as P3HT, showed lower ϕ_F values in thin films than in solution of good solvents. Among the three polymers, photoluminescence quenching was found higher for P3HT, with a ϕ_F decreasing from 0.19 in toluene to 0.009 in thin films [153]. It is interesting to realize that emission quenching, followed by the red-shifted emission spectra in the solid state, was previously attributed to emission from interchain (aggregate) excited states in P3HT films, where symmetry considerations reduce the intensity of the high energy emission [159]. Amongst the poly(TPE-thiophene) polymers, the quenching was found more pronounced for coPT ($\phi_F = 0.22$ in toluene versus $\phi_F = 0.03$ in the solid film—a ratio of ~ 7) than for homoPT (0.13 versus 0.08, a ratio of ~ 1.6). These results suggest that for the PT with a TPE substituent in each thiophene unit, homoPT, the higher steric hindrance reduces planarization of the main backbone polymer chain in the film (although imparting rigidification of the skeketon) and thus the ACQ process is less efficient than for the other polythiophene counterparts. To further study these polymers, lead ACQ compounds in solvent-nonsolvent mixtures were investigated in THF:water mixtures and correlated with the monomer T-TPE (Fig. 11).

For T-TPE, a clear enhancement of the emission band was observed for mixtures with a $f_W \geq 90\%$, thus showing the presence of the AIE effect. For the polymers, a red-shift of the emission was found on going from THF to $f_W = 90\%$ (where the highest degree of aggregation is expected), see Fig. 11. For the coPT and P3HT polymers, ACQ is clearly dominant, starting immediately from very low water fractions, whereas for homoPT, in THF:water mixtures, suppression of fluorescence emission was less pronounced than for coPT; indeed, only a minor gradual decrease of fluorescence was observed up to the mixture with the highest water content. Thus, contrary to what is observed for the coPT polymer, the characteristic thiophene-TPE monomeric unit of the homoPT polymer restricts (although not completely) formation of non-emissive aggregates. This shows that a higher degree of TPE substituents (as in homoPT) restricts formation of non-emissive aggregates, basically balancing the AIE and ACQ effects (Fig. 11).

Another interesting feature coming from the study of these polymers is the observation from time-resolved fluorescence studies, as a function of temperature, that for homoPT and coPT, the deactivation of the excited state occurs mainly through energy migration along the polymer backbone. Moreover, for P3HT, the excited state decay involves competition between conformational relaxation (associated with decay times in the 12.8–15.4 ps range) and energy migration (~ 80 ps) [153]. Again, absence of conformational relaxation for TPE-substituted polythiophenes can be attributed to the restriction of torsional movements promoted by the bulky TPE substituents in these polythiophenes. The study showed that, even though the strategy of incorporation AIE-luminogen into the polymer backbone could not circumvent the ACQ effect in all polythiophenes, restriction in the formation of nonemissive aggregates was observed. Indeed, T-TPE showed AIE, and with homoPT the ACQ and AIE effects apparently cancel each other out [153].

6 Concluding Remarks

In the past 20 years, and associated with the discovery of the AIE effect, a plethora of AIEgen molecules has been developed. The challenges are now in the development of applications to take real advantage of this effect. Despite the enormous number of structures, the rational design of new structures remains a challenge. The future design of innovative AIE systems, small molecules (oligomers) and polymers, will take advantage of known photophysical mechanisms to prevent ACQ phenomena in solid, aggregate or confined media. Despite the enormous number of studies in the past two decades on this effect, of making emissive molecules that, otherwise isolated, are non-emissive, this seems just the beginning of a chapter of exciting new research. The rediscovery of molecules that may suffer structural changes in the excited state (e.g., molecular rigidity or the decrease of the number of low lying vibrational levels by minimizing the contribution via the loose bolt effect) opens a new route for an enormous variety of AIEgens. Additional strategies to increase the photoluminescence emission in the solid, or aggregate state, will surely include the design of J-aggregate forming compounds, molecules with room temperature phosphorescence and thermally activated delayed fluorescence.

Acknowledgements The authors acknowledge financial support from Project "Hylight" (no. 031625) 02/SAICT/2017, PTDC/QUI-QFI/31625/2017, which is funded by the Portuguese Science Foundation (Fundação para Ciência e Tecnologia, FCT) and COMPETE Centro 2020. We also acknowledge funding by Fundo Europeu de Desenvolvimento Regional (FEDER) through COMPETE and project ROTEIRO/0152/2013. The Coimbra Chemistry Centre (CQC) is supported through projects UIDB/00313/2020 and UIDP/00313/2020, co-funded by FCT and COMPETE 2020.

Compliance with Ethical Standards

Conflict of interest The authors declare that there is no conflict of interests.

References

1. Luo J, Xie Z, Lam JW, Cheng L, Chen H, Qiu C, Kwok HS, Zhan X, Liu Y, Zhu D, Tang BZ (2001) Aggregation-induced emission of 1-methyl-1,2,3,4,5-pentaphenylsilole. Chem Commun 18:1740–1741. https://doi.org/10.1039/b105159h
2. Birks JB (1970) Photophysics of aromatic molecules. Wiley, London
3. Tang BZ, Zhan X, Yu G, Sze Lee PP, Liu Y, Zhu D (2001) Efficient blue emission from siloles. J Mat Chem 11(12):2974–2978. https://doi.org/10.1039/b102221k
4. Jenekhe SA, Chen XL (2000) Supramolecular photophysics of self-assembled block copolymers containing luminescent conjugated polymers. J Phys Chem B 104(27):6332–6335. https://doi.org/10.1021/jp000896u
5. Pant DD, Bhagchandani CL, Pant KC, Verma SP (1971) Aggregation in xanthene dyes, exciton emission and phosphorescence enhancement. Chem Phys Lett 9(6):546–547. https://doi.org/10.1016/0009-2614(71)85121-7
6. Winnik FM (1993) Photophysics of preassociated pyrenes in aqueous polymer solutions and in other organized media. Chem Rev 93(2):587–614. https://doi.org/10.1021/cr00018a001
7. Kitamura T, Takahashi Y, Yamanaka T, Uchida K (1991) Luminescence associated with the molecular aggregation of hydrocarbons doped in amorphous silica glasses. J Lumin 48–49:373–376. https://doi.org/10.1016/0022-2313(91)90141-h

8. Rudalevige T, Francis AH, Zand R (1998) Spectroscopic studies of fullerene aggregates. J Phys Chem A 102(48):9797–9802. https://doi.org/10.1021/jp9832591
9. Carter PW, DiMagno SG, Porter JD, Streitwieser A (1993) pi-Stacking and aggregation of pyridinium-substituted indolizin. J Phys Chem 97(5):1085–1096. https://doi.org/10.1021/j100107a017
10. Xu W, Guo H, Akins DL (2001) Aggregation and exciton emission of a cyanine dye encapsulated within mesoporous MCM-41. J Phys Chem B 105(32):7686–7689. https://doi.org/10.1021/jp004154c
11. Möbius D (1995) Scheibe aggregates. Adv Mater 7(5):437–444. https://doi.org/10.1002/adma.19950070503
12. Scheibe G (1937) Über die Veränderlichkeit der Absorptionsspektren in Lösungen und die Nebenvalenzen als ihre Ursache. Angew Chem-Ger Edit 50(11):212–219. https://doi.org/10.1002/ange.19370501103
13. Jelley EE (1936) Spectral absorption and fluorescence of dyes in the molecular state. Nature 138(3502):1009–1010. https://doi.org/10.1038/1381009a0
14. Jelley EE (1937) Molecular, nematic and crystal states of I: I-diethyl–cyanine chloride. Nature 139(3519):631–631. https://doi.org/10.1038/139631b0
15. Wurthner F, Kaiser TE, Saha-Moller CR (2011) J-aggregates: from serendipitous discovery to supramolecular engineering of functional dye materials. Angew Chem Int Ed Engl 50(15):3376–3410. https://doi.org/10.1002/anie.201002307
16. Kasha M, Rawls HR, El-Bayoumi MA (1965) The exciton model in molecular spectroscopy. Pure Appl Chem 11(3–4):371–392. https://doi.org/10.1351/pac196511030371
17. Brixner T, Hildner R, Köhler J, Lambert C, Würthner F (2017) Exciton transport in molecular aggregates—from natural antennas to synthetic chromophore systems. Adv Energy Mater 7:16. https://doi.org/10.1002/aenm.201700236
18. Kasha M (1976) Molecular Excitons in Small Aggregates. In: Di Bartolo B, Pacheco D, Goldberg V (eds) Spectroscopy of the excited state, vol 12, vol NATO Advanced Study Institutes Series (Series B: Physics). Springer, Boston. https://doi.org/10.1007/978-1-4684-2793-6_12
19. Deshmukh AP, Koppel D, Chuang C, Cadena DM, Cao J, Caram JR (2019) Design principles for two-dimensional molecular aggregates using Kasha's Model: tunable photophysics in near and short-wave infrared. J Phys Chem C 123(30):18702–18710. https://doi.org/10.1021/acs.jpcc.9b05060
20. Oelkrug D, Tompert A, Egelhaaf H-J, Hanack M, Steinhuber E, Hohloch M, Meier H, Stalmach U (1996) Towards highly luminescent phenylene vinylene films. Synth Methods 83(3):231–237. https://doi.org/10.1016/s0379-6779(96)04484-0
21. Oelkrug D, Tompert A, Gierschner J, Egelhaaf H-J, Hanack M, Hohloch M, Steinhuber E (1998) Tuning of fluorescence in films and nanoparticles of oligophenylenevinylenes. J Phys Chem B 102(11):1902–1907. https://doi.org/10.1021/jp973225d
22. Choi S, Bouffard J, Kim Y (2014) Aggregation-induced emission enhancement of a meso-trifluoromethyl BODIPY via J-aggregation. Chem Sci 5(2):751–755. https://doi.org/10.1039/c3sc52495g
23. Sheng W, Zheng Y-Q, Wu Q, Chen K, Li M, Jiao L, Hao E, Wang J-Y, Pei J (2020) Synthesis, characterization, and tunable semiconducting properties of aza-BODIPY derived polycyclic aromatic dyes. Sci China Chem 63(9):1240–1245. https://doi.org/10.1007/s11426-020-9807-7
24. Dong Y, Lam JWY, Qin A, Li Z, Sun J, Kwok HS, Tang BZ (2006) Aggregation-induced emission, vol 6333. SPIE optics + photonics. SPIE, Bellingham WA. https://doi.org/10.1117/12.679373
25. Tong H, Dong Y, Haussler M, Lam JW, Sung HH, Williams ID, Sun J, Tang BZ (2006) Tunable aggregation-induced emission of diphenyldibenzofulvenes. Chem Commun 10:1133–1135. https://doi.org/10.1039/b515798f
26. Dong Y, Lam JW, Qin A, Li Z, Sun J, Sung HH, Williams ID, Tang BZ (2007) Switching the light emission of (4-biphenylyl)phenyldibenzofulvene by morphological modulation: crystallization-induced emission enhancement. Chem Commun 1:40–42. https://doi.org/10.1039/b613157c
27. Ren Y, Lam JW, Dong Y, Tang BZ, Wong KS (2005) Enhanced emission efficiency and excited state lifetime due to restricted intramolecular motion in silole aggregates. J Phys Chem B 109(3):1135–1140. https://doi.org/10.1021/jp046659z
28. Wurthner F (2020) Aggregation-induced emission (AIE): a historical perspective. Angew Chem Int Ed Engl 59(34):14192–14196. https://doi.org/10.1002/anie.202007525
29. Valeur B, Berberan-Santos MN (2012) Structural effects on fluorescence emission. In: Molecular fluorescence. Wiley, New York, pp 75–107. https://doi.org/10.1002/9783527650002.ch4

30. Takezaki M, Hirota N, Terazima M (1996) Excited state dynamics of 9,10-diazaphenanthrene studied by the time-resolved transient grating method. J Phys Chem 100(24):10015–10020. https://doi.org/10.1021/jp9602540
31. Tabuchi M, Momotake A, Kanna Y, Nishimura Y, Arai T (2011) Extremely efficient and long lifetime fluorescence of cis-stilbene contained in a rigid dendrimer. Photochem Photobiol Sci 10(10):1521–1523. https://doi.org/10.1039/C1PP05126A
32. Saltiel J, Megarity ED, Kneipp KG (1966) The mechanism of direct CIS-trans photoisomerization of the stilbenes. J Am Chem Soc 88(10):2336–2338. https://doi.org/10.1021/ja00962a057
33. Charlton JL, Saltiel J (1977) An analysis of trans-stilbene fluorescence quantum yields and lifetimes. J Phys Chem 81(20):1940–1944. https://doi.org/10.1021/j100535a011
34. Saltiel J, Zafiriou OC, Megarity ED, Lamola AA (1968) Tests of the singlet mechanism for cis-trans photoisomerization of the stilbenes. J Am Chem Soc 90(17):4759. https://doi.org/10.1021/ja01019a063
35. DeBoer CD, Schlessinger RH (1968) Multiplicity of the photochemically reactive state of 1,2-diphenylcyclobutene. J Am Chem Soc 90(3):803–804. https://doi.org/10.1021/ja01005a052
36. Valeur B (2002) Molecular fluorescence: principles and applications. Wiley, Weinheim
37. Tsin ATC, Pedrozo-Fernandez HA, Gallas JM, Chambers JP (1988) The fluorescence quantum yield of vitamin A2. Life Sci 43(17):1379–1384. https://doi.org/10.1016/0024-3205(88)90304-9
38. Schoof S, Güsten H, Von Sonntag C (1978) Fluoreszenz und Fluoreszenzlöschung von meso-substituierten Anthracenderivaten in Lösung. Berichte Bunsengesellschaft Phys Chem. 82(10):1068–1073. https://doi.org/10.1002/bbpc.19780821009
39. Guesten H, Mintas M, Klasinc L (1980) Deactivation of the fluorescent state of 9-tert-butylanthracene. 9-tert-Butyl-9,10(Dewar anthracene). J Am Chem Soc 102(27):7936–7937. https://doi.org/10.1021/ja00547a022
40. Jiao L, Yu C, Wang J, Briggs EA, Besley NA, Robinson D, Ruedas-Rama MJ, Orte A, Crovetto L, Talavera EM, Alvarez-Pez JM, Van der Auweraer M, Boens N (2015) Unusual spectroscopic and photophysical properties of meso-tert-butylBODIPY in comparison to related alkylated BODIPY dyes. RSC Adv 5(109):89375–89388. https://doi.org/10.1039/C5RA17419H
41. Zhang H, Liu J, Du L, Ma C, Leung NLC, Niu Y, Qin A, Sun J, Peng Q, Sung HHY, Williams ID, Kwok RTK, Lam JWY, Wong KS, Phillips DL, Tang BZ (2019) Drawing a clear mechanistic picture for the aggregation-induced emission process. Mater Chem Front 3(6):1143–1150. https://doi.org/10.1039/C9QM00156E
42. Dong Y, Lam JWY, Qin A, Liu J, Li Z, Tang BZ, Sun J, Kwok HS (2007) Aggregation-induced emissions of tetraphenylethene derivatives and their utilities as chemical vapor sensors and in organic light-emitting diodes. Appl Phys Lett 91:1. https://doi.org/10.1063/1.2753723
43. Tanaka Y, Machida T, Noumi T, Sada K, Kokado K (2020) Emissive tetraphenylethylene (TPE) derivatives in a dissolved state tightly fastened by a short oligo(ethylene glycol) chain. Org Chem Front 7(18):2649–2656. https://doi.org/10.1039/d0qo00839g
44. Stegemeyer H (1968) Luminescence of sterically hindered arylethylenes. Ber Bunsen Phys Chem 72(2):335–340. https://doi.org/10.1002/bbpc.19680720264
45. Fischer G, Fischer E, Stegemeyer H (1973) Fluorescence and absorption spectra of sterically hindered arylethylenes in the neat glassy state. Ber Bunsen Phys Chem 77(9):685–687. https://doi.org/10.1002/bbpc.19730770907
46. Leigh WJ, Arnold DR (1981) Merostabilization in radical ions, triplets, and biradicals. 6. The excited state behaviour of para-substituted tetraphenylethylenes. Can J Chem 59(21):3061–3075. https://doi.org/10.1139/v81-448
47. Sharafy S, Muszkat KA (1971) Viscosity dependence of fluorescence quantum yields. J Am Chem Soc 93(17):4119–4125. https://doi.org/10.1021/ja00746a004
48. Klingenberg HH, Lippert E, Rapp W (1973) The influence of an intramolecular relaxation process on the frequency-time behaviour or the fluorescence of tetraphenylethylene in highly viscous solutions. Chem Phys Lett 18(3):417–419. https://doi.org/10.1016/0009-2614(73)80206-4
49. Barbara PF, Rand SD, Rentzepis PM (1981) Direct measurements of tetraphenylethylene torsional motion by picosecond spectroscopy. J Am Chem Soc 103(9):2156–2162. https://doi.org/10.1021/ja00399a003
50. Greene BI (1981) Observation of a long-lived twisted intermediate following picosecond UV excitation of tetraphenylethylene. Chem Phys Lett 79(1):51–53. https://doi.org/10.1016/0009-2614(81)85286-4

51. Zijlstra RWJ, van Duijnen PT, Feringa BL, Steffen T, Duppen K, Wiersma DA (1997) Excited-state dynamics of tetraphenylethylene: ultrafast stokes shift, isomerization, and charge separation. J Phys Chem A 101(51):9828–9836. https://doi.org/10.1021/jp971763k
52. Turro NJ (1991) Modern molecular photochemistry. University Science Books, Mill Valley
53. Becker RS (1969) Theory and interpretation of fluorescence and phosphorescence. Wiley, New York
54. Xu S, Duan Y, Liu B (2020) Precise molecular design for high-performance luminogens with aggregation-induced emission. Adv Mater 32(1):e1903530. https://doi.org/10.1002/adma.201903530
55. Yang J, Chi Z, Zhu W, Tang BZ, Li Z (2019) Aggregation-induced emission: a coming-of-age ceremony at the age of eighteen. Sci China Chem 62(9):1090–1098. https://doi.org/10.1007/s11426-019-9512-x
56. Hu R, Qin A, Tang BZ (2020) AIE polymers: synthesis and applications. Prog Polym Sci. https://doi.org/10.1016/j.progpolymsci.2019.101176
57. Zhou S-Y, Wan H-B, Zhou F, Gu P-Y, Xu Q-F, Lu J-M (2019) AIEgens-lightened functional polymers: synthesis, properties and applications. Chin J Polym Sci 37(4):302–326. https://doi.org/10.1007/s10118-019-2217-0
58. Li J, Wang J, Li H, Song N, Wang D, Tang BZ (2020) Supramolecular materials based on AIE luminogens (AIEgens): construction and applications. Chem Soc Rev 49(4):1144–1172. https://doi.org/10.1039/c9cs00495e
59. Pina J, Pinheiro D, Nascimento B, Pineiro M, Seixas de Melo JS (2014) The effect of polyaromatic hydrocarbons on the spectral and photophysical properties of diaryl-pyrrole derivatives: an experimental and theoretical study. Phys Chem Chem Phys 16(34):18319–18326. https://doi.org/10.1039/c4cp01797h
60. Chang D, Chen J, Liu Y, Huang H, Qin A, Deng GJ (2021) Metal-free synthesis and photophysical properties of 1,2,4-triarylpyrroles. J Org Chem 86:110–127 https://doi.org/10.1021/acs.joc.0c01788
61. Chen M, Li L, Wu H, Pan L, Li S, He B, Zhang H, Sun JZ, Qin A, Tang BZ (2018) Unveiling the different emission behavior of polytriazoles constructed from pyrazine-based AIE monomers by click polymerization. ACS Appl Mater Interfaces 10(15):12181–12188. https://doi.org/10.1021/acsami.8b03178
62. Guo Z, Yan C, Zhu W-H (2020) High-performance quinoline-malononitrile core as a building block for the diversity-oriented synthesis of AIEgens. Angew Chem Int Ed Engl 59(25):9812–9825. https://doi.org/10.1002/anie.201913249
63. Qian Y, Cai MM, Xie LH, Yang GQ, Wu SK, Huang W (2011) Restriction of photoinduced twisted intramolecular charge transfer. ChemPhysChem 12(2):397–404. https://doi.org/10.1002/cphc.201000457
64. Zhou P, Li P, Zhao Y, Han K (2019) Restriction of flip-flop motion as a mechanism for aggregation-induced emission. J Phys Chem Lett 10(21):6929–6935. https://doi.org/10.1021/acs.jpclett.9b02922
65. Yin PA, Wan Q, Niu Y, Peng Q, Wang Z, Li Y, Qin A, Shuai Z, Tang BZ (2020) Theoretical and experimental investigations on the aggregation-enhanced emission from dark state: vibronic coupling effect. Adv Electron Mater 6:7. https://doi.org/10.1002/aelm.202000255
66. Hong Y, Lam JW, Tang BZ (2009) Aggregation-induced emission: phenomenon, mechanism and applications. Chem Commun 29:4332–4353. https://doi.org/10.1039/b904665h
67. Mei J, Hong Y, Lam JW, Qin A, Tang Y, Tang BZ (2014) Aggregation-induced emission: the whole is more brilliant than the parts. Adv Mater 26(31):5429–5479. https://doi.org/10.1002/adma.201401356
68. Leung NLC, Xie N, Yuan W, Liu Y, Wu Q, Peng Q, Miao Q, Lam JWY, Tang BZ (2014) Restriction of intramolecular motions: the general mechanism behind aggregation-induced emission. Chem Eur J 20(47):15349–15353. https://doi.org/10.1002/chem.201403811
69. Mazzucato U, Spalletti A (2009) Competition between photoisomerization and photocyclization of the cis isomers of n-styrylnaphthalenes and -phenanthrenes. J Phys Chem A 113(52):14521–14529. https://doi.org/10.1021/jp904017e
70. Prlj A, Doslic N, Corminboeuf C (2016) How does tetraphenylethylene relax from its excited states? Phys Chem Chem Phys 18(17):11606–11609. https://doi.org/10.1039/c5cp04546k
71. Gao YJ, Chang XP, Liu XY, Li QS, Cui G, Thiel W (2017) Excited-state decay paths in tetraphenylethene derivatives. J Phys Chem A 121(13):2572–2579. https://doi.org/10.1021/acs.jpca.7b00197

72. Gao BR, Wang HY, Hao YW, Fu LM, Fang HH, Jiang Y, Wang L, Chen QD, Xia H, Pan LY, Ma YG, Sun HB (2010) Time-resolved fluorescence study of aggregation-induced emission enhancement by restriction of intramolecular charge transfer state. J Phys Chem B 114(1):128–134. https://doi.org/10.1021/jp909063d
73. Sasaki S, Drummen GPC, Konishi G-i (2016) Recent advances in twisted intramolecular charge transfer (TICT) fluorescence and related phenomena in materials chemistry. J Mater Chem C 4(14):2731–2743. https://doi.org/10.1039/c5tc03933a
74. Liu J, Zhang C, Dong J, Zhu J, Shen C, Yang G, Zhang X (2017) Endowing a triarylboron compound showing ACQ with AIE characteristics by transforming its emissive TICT state to be dark. RSC Adv 7(24):14511–14515. https://doi.org/10.1039/c7ra00426e
75. Tseng N-W, Liu J, Ng JCY, Lam JWY, Sung HHY, Williams ID, Tang BZ (2012) Deciphering mechanism of aggregation-induced emission (AIE): Is E-Zisomerisation involved in an AIE process? Chem Sci 3(2):493–497. https://doi.org/10.1039/c1sc00690h
76. Garg K, Ganapathi E, Rajakannu P, Ravikanth M (2015) Stereochemical modulation of emission behaviour in E/Z isomers of diphenyldipyrroethene from aggregation induced emission to crystallization induced emission. Phys Chem Chem Phys 17(29):19465–19473. https://doi.org/10.1039/c5cp02400e
77. Yang Z, Qin W, Leung NLC, Arseneault M, Lam JWY, Liang G, Sung HHY, Williams ID, Tang BZ (2016) A mechanistic study of AIE processes of TPE luminogens: intramolecular rotation vs configurational isomerization. J Mater Chem C 4(1):99–107. https://doi.org/10.1039/c5tc02924d
78. Xie Y, Li Z (2019) Recent advances in the Z/E isomers of tetraphenylethene derivatives: stereoselective synthesis, AIE mechanism, photophysical properties, and application as chemical probes. Chem Asian J 14(15):2524–2541. https://doi.org/10.1002/asia.201900282
79. Stojanović L, Crespo-Otero R (2019) Understanding aggregation induced emission in a propeller-shaped blue emitter. ChemPhotoChem 3(9):907–915. https://doi.org/10.1002/cptc.201900075
80. Xu Y, Wang F, Chen X, Liu Y, Zhou Z, Teng B (2019) A new strategy of design and development of aggregation-induced emission materials based on a deep insight into mechanism. J Phys Chem C 123(48):29379–29385. https://doi.org/10.1021/acs.jpcc.9b06198
81. Suzuki S, Sasaki S, Sairi AS, Iwai R, Tang BZ, Konishi G-i (2020) Principles of aggregation-induced emission: design of deactivation pathways for advanced AIEgens and applications. Angew Chem Int Ed Engl 59(25):9856–9867. https://doi.org/10.1002/anie.202000940
82. Kokado K, Sada K (2019) Consideration of molecular structure in the excited state to design new luminogens with aggregation-induced emission. Angew Chem Int Ed Engl 58(26):8632–8639. https://doi.org/10.1002/anie.201814462
83. Tu Y, Liu J, Zhang H, Peng Q, Lam JWY, Tang BZ (2019) Restriction of access to the dark state: a new mechanistic model for heteroatom-containing AIE systems. Angew Chem Int Ed Engl 58(42):14911–14914. https://doi.org/10.1002/anie.201907522
84. Crespo-Otero R, Li Q, Blancafort L (2019) Exploring potential energy surfaces for aggregation-induced emission—from solution to crystal. Chem Asian J 14(6):700–714. https://doi.org/10.1002/asia.201801649
85. Li Q, Blancafort L (2013) A conical intersection model to explain aggregation induced emission in diphenyl dibenzofulvene. Chem Commun 49(53):5966–5968. https://doi.org/10.1039/C3CC41730A
86. Peng X-L, Ruiz-Barragan S, Li Z-S, Li Q-S, Blancafort L (2016) Restricted access to a conical intersection to explain aggregation induced emission in dimethyl tetraphenylsilole. J Mater Chem C 4(14):2802–2810. https://doi.org/10.1039/C5TC03322E
87. Suzuki S, Maeda S, Morokuma K (2015) Exploration of quenching pathways of multiluminescent acenes using the GRRM method with the SF-TDDFT method. J Phys Chem A 119(47):11479–11487. https://doi.org/10.1021/acs.jpca.5b07682
88. Kokado K, Machida T, Iwasa T, Taketsugu T, Sada K (2018) Twist of C=C bond plays a crucial role in the quenching of AIE-active tetraphenylethene derivatives in solution. J Phys Chem C 122(1):245–251. https://doi.org/10.1021/acs.jpcc.7b11248
89. Yoshii R, Nagai A, Tanaka K, Chujo Y (2013) Highly emissive boron ketoiminate derivatives as a new class of aggregation-induced emission fluorophores. Chem Eur J 19(14):4506–4512. https://doi.org/10.1002/chem.201203703
90. Nie H, Hu K, Cai Y, Peng Q, Zhao Z, Hu R, Chen J, Su S-J, Qin A, Tang BZ (2017) Tetraphenylfuran: aggregation-induced emission or aggregation-caused quenching? Mater Chem Front 1(6):1125–1129. https://doi.org/10.1039/C6QM00343E

91. Baig MZK, Prusti B, Roy D, Chakravarty M (2019) Positional variation of monopyridyl-N in unsymmetrical anthracenyl pi-conjugates: difference between solution- and aggregate-state emission behavior. ACS Omega 4(3):5052–5063. https://doi.org/10.1021/acsomega.9b00046
92. Tang Y, Tang BZ (2019) Principles and applications of aggregation-induced emission. Springer, Berlin. https://doi.org/10.1007/978-3-319-99037-8
93. Wang Y, Liu T, Bu L, Li J, Yang C, Li X, Tao Y, Yang W (2012) Aqueous nanoaggregation-enhanced one- and two-photon fluorescence, crystalline J-aggregation-induced red shift, and amplified spontaneous emission of 9,10-bis(p-dimethylaminostyryl)anthracene. J Phys Chem C 116(29):15576–15583. https://doi.org/10.1021/jp3031094
94. Zhou J, Chang Z, Jiang Y, He B, Du M, Lu P, Hong Y, Kwok HS, Qin A, Qiu H, Zhao Z, Tang BZ (2013) From tetraphenylethene to tetranaphthylethene: structural evolution in AIE luminogen continues. Chem Commun 49(25):2491–2493. https://doi.org/10.1039/C3CC00010A
95. Wang J, Mei J, Hu R, Sun JZ, Qin A, Tang BZ (2012) Click synthesis, aggregation-induced emission, E/Z isomerization, self-organization, and multiple chromisms of pure stereoisomers of a tetraphenylethene-cored luminogen. J Am Chem Soc 134(24):9956–9966. https://doi.org/10.1021/ja208883h
96. Zhang G-F, Chen Z-Q, Aldred MP, Hu Z, Chen T, Huang Z, Meng X, Zhu M-Q (2014) Direct validation of the restriction of intramolecular rotation hypothesis via the synthesis of novel ortho-methyl substituted tetraphenylethenes and their application in cell imaging. Chem Commun 50(81):12058–12060. https://doi.org/10.1039/C4CC04241G
97. Zhang G-F, Wang H, Aldred MP, Chen T, Chen Z-Q, Meng X, Zhu M-Q (2014) General synthetic approach toward geminal-substituted tetraarylethene fluorophores with tunable emission properties: X-ray crystallography. Aggreg Induced Emiss Piezofluorochrom Chem Mater 26(15):4433–4446. https://doi.org/10.1021/cm501414b
98. Rodrigues ACB, Geisler IS, Klein P, Pina J, Neuhaus FJH, Dreher E, Lehmann CW, Scherf U, Seixas de Melo JS (2020) Designing highly fluorescent, arylated poly(phenylene vinylene)s of intrinsic microporosity. J Mater Chem C 8(7):2248–2257. https://doi.org/10.1039/c9tc06028f
99. Cai Y, Du L, Samedov K, Gu X, Qi F, Sung HHY, Patrick BO, Yan Z, Jiang X, Zhang H, Lam JWY, Williams ID, Lee Phillips D, Qin A, Tang BZ (2018) Deciphering the working mechanism of aggregation-induced emission of tetraphenylethylene derivatives by ultrafast spectroscopy. Chem Sci 9(20):4662–4670. https://doi.org/10.1039/C8SC01170B
100. Dong YQ, Lam JW, Tang BZ (2015) Mechanochromic luminescence of aggregation-induced emission luminogens. J Phys Chem Lett 6(17):3429–3436. https://doi.org/10.1021/acs.jpclett.5b01090
101. Duan Y, Ma H, Tian H, Liu J, Deng X, Peng Q, Dong YQ (2019) Construction of a luminogen exhibiting high contrast and multicolored emission switching through combination of a bulky conjugation core and tolyl groups. Chem Asian J 14(6):864–870. https://doi.org/10.1002/asia.201801608
102. Dong Y, Lam JWY, Li Z, Qin A, Tong H, Dong Y, Feng X, Tang BZ (2005) Vapochromism of hexaphenylsilole. J Inorg Organomet 15(2):287–291. https://doi.org/10.1007/s10904-005-5546-0
103. Zheng M, Sun M, Li Y, Wang J, Bu L, Xue S, Yang W (2014) Piezofluorochromic properties of AIE-active 9,10-bis(N-alkylpheno-thiazin-3-yl-vinyl-2)anthracenes with different length of alkyl chains. Dyes Pigments 102:29–34. https://doi.org/10.1016/j.dyepig.2013.10.020
104. Zhang G, Sun J, Xue P, Zhang Z, Gong P, Peng J, Lu R (2015) Phenothiazine modified triphenylacrylonitrile derivates: AIE and mechanochromism tuned by molecular conformation. J Mater Chem C 3(12):2925–2932. https://doi.org/10.1039/c4tc02925a
105. Huang B, Chen WC, Li Z, Zhang J, Zhao W, Feng Y, Tang BZ, Lee CS (2018) Manipulation of molecular aggregation states to realize polymorphism, AIE, MCL, and TADF in a single molecule. Angew Chem Int Ed Engl 57(38):12473–12477. https://doi.org/10.1002/anie.201806800
106. Luo X, Li J, Li C, Heng L, Dong YQ, Liu Z, Bo Z, Tang BZ (2011) Reversible switching of the emission of diphenyldibenzofulvenes by thermal and mechanical stimuli. Adv Mater 23(29):3261–3265. https://doi.org/10.1002/adma.201101059
107. Zhao J, Chi Z, Zhang Y, Mao Z, Yang Z, Ubba E, Chi Z (2018) Recent progress in the mechanofluorochromism of cyanoethylene derivatives with aggregation-induced emission. J Mater Chem C 6(24):6327–6353. https://doi.org/10.1039/c8tc01648h
108. Yang Z, Chi Z, Mao Z, Zhang Y, Liu S, Zhao J, Aldred MP, Chi Z (2018) Recent advances in mechano-responsive luminescence of tetraphenylethylene derivatives with aggregation-induced emission properties. Mater Chem Front 2(5):861–890. https://doi.org/10.1039/c8qm00062j

109. Ubba E, Tao Y, Yang Z, Zhao J, Wang L, Chi Z (2018) Organic mechanoluminescence with aggregation-induced emission. Chem Asian J 13(21):3106–3121. https://doi.org/10.1002/asia.201800926
110. Zhao J, Chi Z, Yang Z, Mao Z, Zhang Y, Ubba E, Chi Z (2018) Recent progress in the mechanofluorochromism of distyrylanthracene derivatives with aggregation-induced emission. Mater Chem Front 2(9):1595–1608. https://doi.org/10.1039/c8qm00130h
111. Lin Y, Chen G, Zhao L, Yuan WZ, Zhang Y, Tang BZ (2015) Diethylamino functionalized tetraphenylethenes: structural and electronic modulation of photophysical properties, implication for the CIE mechanism and application to cell imaging. J Mater Chem C 3(1):112–120. https://doi.org/10.1039/c4tc02161d
112. Yang J, Gao X, Xie Z, Gong Y, Fang M, Peng Q, Chi Z, Li Z (2017) Elucidating the excited state of mechanoluminescence in organic luminogens with room-temperature phosphorescence. Angew Chem Int Ed Engl 56(48):15299–15303. https://doi.org/10.1002/anie.201708119
113. Xue P, Ding J, Chen P, Wang P, Yao B, Sun J, Sun J, Lu R (2016) Mechanical force-induced luminescence enhancement and chromism of a nonplanar D–A phenothiazine derivative. J Mater Chem C 4(23):5275–5280. https://doi.org/10.1039/c6tc01193d
114. Ma C, Zhang X, Yang Y, Ma Z, Yang L, Wu Y, Liu H, Jia X, Wei Y (2016) Halogen effect on mechanofluorochromic properties of alkyl phenothiazinyl phenylacrylonitrile derivatives. Dyes Pigments 129:141–148. https://doi.org/10.1016/j.dyepig.2016.02.028
115. Yang J, Qin J, Geng P, Wang J, Fang M, Li Z (2018) Molecular conformation-dependent mechanoluminescence: same mechanical stimulus but different emissive color over time. Angew Chem Int Ed Engl 57(43):14174–14178. https://doi.org/10.1002/anie.201809463
116. Chen Y, Xu C, Xu B, Mao Z, Li J-A, Yang Z, Peethani NR, Liu C, Shi G, Gu FL, Zhang Y, Chi Z (2019) Chirality-activated mechanoluminescence from aggregation-induced emission enantiomers with high contrast mechanochromism and force-induced delayed fluorescence. Mater Chem Front 3(9):1800–1806. https://doi.org/10.1039/c9qm00312f
117. Massie SP (1954) The chemistry of phenothiazine. Chem Rev 54(5):797–833. https://doi.org/10.1021/cr60171a003
118. El- Sayed MA (1968) Triplet state—its radiative and nonradiative properties. Accounts Chem Res 1(1):8–16
119. Okazaki M, Takeda Y, Data P, Pander P, Higginbotham H, Monkman AP, Minakata S (2017) Thermally activated delayed fluorescent phenothiazine–dibenzo[a, j]phenazine–phenothiazine triads exhibiting tricolor-changing mechanochromic luminescence. Chem Sci 8(4):2677–2686. https://doi.org/10.1039/c6sc04863c
120. Nobuyasu RS, Ward JS, Gibson J, Laidlaw BA, Ren Z, Data P, Batsanov AS, Penfold TJ, Bryce MR, Dias FB (2019) The influence of molecular geometry on the efficiency of thermally activated delayed fluorescence. J Mater Chem C 7(22):6672–6684. https://doi.org/10.1039/c9tc00720b
121. Wagner E, Filipek S, Kalinowski MK (1988) Visible absorption spectra of the phenothiazine radical cation and its 10-substituted derivatives. Monatsh Chem 119(8–9):929–932
122. Huang L, Wen X, Liu J, Chen M, Ma Z, Jia X (2019) An AIE molecule featuring changeable triplet emission between phosphorescence and delayed fluorescence by an external force. Mater Chem Front 3(10):2151–2156. https://doi.org/10.1039/c9qm00509a
123. Shi R, Chen H, Qi Y, Huang W, Yin G, Wang R (2019) From aggregation-induced to solution emission: a new strategy for designing ratiometric fluorescent probes and its application for in vivo HClO detection. Analyst 144(5):1696–1703. https://doi.org/10.1039/c8an01950a
124. Gong J, Han J, Liu Q, Ren X, Wei P, Yang L, Zhang Y, Liu J, Dong Y, Wang Y, Song X, Tang BZ (2019) An ideal platform of light-emitting materials from phenothiazine: facile preparation, tunable red/NIR fluorescence, bent geometry-promoted AIE behaviour and selective lipid-droplet (LD) tracking ability. J Mater Chem C 7(14):4185–4190. https://doi.org/10.1039/c9tc00143c
125. Rodrigues ACB, Pina J, Seixas de Melo JS (2020) Structure-relation properties of N-substituted phenothiazines in solution and solid state: Photophysical, photostability and aggregation-induced emission studies. J Mol Liq 317:113966. https://doi.org/10.1016/j.molliq.2020.113966
126. Jia XR, Yu HJ, Chen J, Gao WJ, Fang JK, Qin YS, Hu XK, Shao G (2018) Stimuli-responsive properties of aggregation-induced-emission compounds containing a 9,10-distyrylanthracene moiety. Chem Eur J 24(71):19053–19059. https://doi.org/10.1002/chem.201804315
127. Freudenberg J, Rominger F, Bunz UH (2015) New aggregation-induced emitters: tetraphenyldistyrylbenzenes. Chem Eur J 21(47):16749–16753. https://doi.org/10.1002/chem.201502877

128. Zhang J, Ma S, Fang H, Xu B, Sun H, Chan I, Tian W (2017) Insights into the origin of aggregation enhanced emission of 9,10-distyrylanthracene derivatives. Mater Chem Front 1(7):1422–1429. https://doi.org/10.1039/C7QM00032D
129. Tong H, Dong Y, Hong Y, Häussler M, Lam JWY, Sung HHY, Yu X, Sun J, Williams ID, Kwok HS, Tang BZ (2007) Aggregation-induced emission: effects of molecular structure, solid-state conformation, and morphological packing arrangement on light-emitting behaviors of diphenyldibenzofulvene derivatives. J Phys Chem C 111(5):2287–2294. https://doi.org/10.1021/jp0630828
130. Gong Y, Tan Y, Liu J, Lu P, Feng C, Yuan WZ, Lu Y, Sun JZ, He G, Zhang Y (2013) Twisted D-pi-A solid emitters: efficient emission and high contrast mechanochromism. Chem Commun 49(38):4009–4011. https://doi.org/10.1039/c3cc39243k
131. Yuan WZ, Gong Y, Chen S, Shen XY, Lam JWY, Lu P, Lu Y, Wang Z, Hu R, Xie N, Kwok HS, Zhang Y, Sun JZ, Tang BZ (2012) Efficient solid emitters with aggregation-induced emission and intramolecular charge transfer characteristics: molecular design, synthesis, photophysical behaviors, and OLED application. Chem Mater 24(8):1518–1528. https://doi.org/10.1021/cm300416y
132. Yuan WZ, Tan Y, Gong Y, Lu P, Lam JW, Shen XY, Feng C, Sung HH, Lu Y, Williams ID, Sun JZ, Zhang Y, Tang BZ (2013) Synergy between twisted conformation and effective intermolecular interactions: strategy for efficient mechanochromic luminogens with high contrast. Adv Mater 25(20):2837–2843. https://doi.org/10.1002/adma.201205043
133. Dong W, Pina J, Pan Y, Preis E, Seixas de Melo JS, Scherf U (2015) Polycarbazoles and polytriphenylamines showing aggregation-induced emission (AIE) and intramolecular charge transfer (ICT) behavior for the optical detection of nitroaromatic compounds. Polymer 76:173–181. https://doi.org/10.1016/j.polymer.2015.08.064
134. Su X, Gao Q, Wang D, Han T, Tang BZ (2020) One-step multicomponent polymerizations for the synthesis of multifunctional AIE polymers. Macromol Rapid Commun. https://doi.org/10.1002/marc.202000471
135. Liu J, Lam JWY, Tang BZ (2009) Aggregation-induced emission of silole molecules and polymers: fundamental and applications. J Inorg Organomet 19(3):249. https://doi.org/10.1007/s10904-009-9282-8
136. Qin A, Lam JWY, Tang BZ (2012) Luminogenic polymers with aggregation-induced emission characteristics. Prog Polym Sci 37(1):182–209. https://doi.org/10.1016/j.progpolymsci.2011.08.002
137. Li Y, Liu S, Han T, Zhang H, Chuah C, Kwok RTK, Lam JWY, Tang BZ (2019) Sparks fly when AIE meets with polymers. Mater Chem Front 3(11):2207–2220. https://doi.org/10.1039/c9qm00404a
138. Qiu Z, Liu X, Lam JWY, Tang BZ (2019) The marriage of aggregation-induced emission with polymer science. Macromol Rapid Commun 40(1):e1800568. https://doi.org/10.1002/marc.201800568
139. Pucci A (2019) Mechanochromic fluorescent polymers with aggregation-induced emission features. Sensors 19:22. https://doi.org/10.3390/s19224969
140. Zhan R, Pan Y, Manghnani PN, Liu B (2017) AIE polymers: synthesis, properties, and biological applications. Macromol Biosci 17:5. https://doi.org/10.1002/mabi.201600433
141. Zhou H, Chua MH, Tang BZ, Xu J (2019) Aggregation-induced emission (AIE)-active polymers for explosive detection. Polym Chem 10(28):3822–3840. https://doi.org/10.1039/c9py00322c
142. Rodrigues ACB, Pina J, Dong W, Forster M, Scherf U, Seixas de Melo JS (2018) Aggregation-induced emission in phenothiazine–TPE and −TPAN polymers. Macromolecules 51(21):8501–8512. https://doi.org/10.1021/acs.macromol.8b01758
143. Gao B-R, Wang H-Y, Yang Z-Y, Wang H, Wang L, Jiang Y, Hao Y-W, Chen Q-D, Li Y-P, Ma Y-G, Sun H-B (2011) Comparative time-resolved study of two aggregation-induced emissive molecules. J Phys Chem C 115(32):16150–16154. https://doi.org/10.1021/jp2027753
144. Hoyt JM, Frank CE, Koch K (1967) Polymerization of bis(α-Haloalkyl) aromatic compounds
145. Baysec S, Preis E, Allard S, Scherf U (2016) Very high solid state photoluminescence quantum yields of poly(tetraphenylethylene) derivatives. Macromol Rapid Commun 37(22):1802–1806. https://doi.org/10.1002/marc.201600485
146. Dalapati S, Gu C, Jiang D (2016) Luminescent porous polymers based on aggregation-induced mechanism: design. Synth Funct Small 12(47):6513–6527. https://doi.org/10.1002/smll.201602427
147. Jansen JC, Esposito E, Fuoco A, Carta M (2019) Microporous organic polymers: synthesis, characterization, and applications. Polymers (Basel) 11:5. https://doi.org/10.3390/polym11050844

148. Patra A, Scherf U (2012) Fluorescent microporous organic polymers: potential testbed for optical applications. Chem Eur J 18(33):10074–10080. https://doi.org/10.1002/chem.201200804
149. Palma-Cando A, Woitassek D, Brunklaus G, Scherf U (2017) Luminescent tetraphenylethene-cored, carbazole- and thiophene-based microporous polymer films for the chemosensing of nitroaromatic analytes. Mater Chem Front 1(6):1118–1124. https://doi.org/10.1039/c6qm00281a
150. Pina J, Seixas de Melo J, Burrows HD, Bilge A, Farrell T, Forster M, Scherf U (2006) Spectral and photophysical studies on cruciform oligothiophenes in solution and the solid state. J Phys Chem B 110(31):15100–15106. https://doi.org/10.1021/jp060707t
151. De Nisi F, Francischello R, Battisti A, Panniello A, Fanizza E, Striccoli M, Gu X, Leung NLC, Tang BZ, Pucci A (2017) Red-emitting AIEgen for luminescent solar concentrators. Mater Chem Front 1(7):1406–1412. https://doi.org/10.1039/c7qm00008a
152. Zhang Z, Liao M, Lou H, Hu Y, Sun X, Peng H (2018) Conjugated polymers for flexible energy harvesting and storage. Adv Mater 30(13):e1704261. https://doi.org/10.1002/adma.201704261
153. Pina J, Rodrigues ACB, Alnady M, Dong W, Scherf U, Seixas de Melo JS (2020) Restricted aggregate formation on tetraphenylethene-substituted polythiophenes. J Phys Chem C 124(25):13956–13965. https://doi.org/10.1021/acs.jpcc.9b10908
154. Raithel D, Baderschneider S, de Queiroz TB, Lohwasser R, Köhler J, Thelakkat M, Kümmel S, Hildner R (2016) Emitting species of poly(3-hexylthiophene): from single. Isolated Chains Bulk Macromol 49(24):9553–9560. https://doi.org/10.1021/acs.macromol.6b02077
155. Becker RS, Seixas de Melo JS, Maçanita AL, Elisei F (1996) Comprehensive evaluation of the absorption, photophysical, energy transfer, structural, and theoretical properties of α-oligothiophenes with one to seven rings. J Phys Chem 100(48):18683–18695. https://doi.org/10.1021/jp960852e
156. Pina J, Burrows HD, Becker RS, Dias FB, Maçanita AL, Seixas de Melo JS (2006) Photophysical Studies of α, ω-dicyano-oligothiophenes NC($_{C}$4$_{H}$2S$_{)}$nCN (n = 1–6). J Phys Chem B 110(13):6499–6505. https://doi.org/10.1021/jp055455v
157. Pina J, Seixas de Melo JS, Burrows HD, Maçanita AL, Galbrecht F, Bünnagel T, Scherf U (2009) Alternating binaphthyl−thiophene copolymers: synthesis, spectroscopy, and photophysics and their relevance to the question of energy migration versus conformational relaxation. Macromolecules 42(5):1710–1719. https://doi.org/10.1021/ma802395c
158. Pina J, Eckert A, Scherf U, Galvão AM, Seixas de Melo JS (2018) Cyclopentadithiophene derivatives: a step towards an understanding of thiophene copolymer excited state deactivation pathways. Mater Chem Front 2(1):149–156. https://doi.org/10.1039/C7QM00440K
159. Clark J, Silva C, Friend RH, Spano FC (2007) Role of intermolecular coupling in the photophysics of disordered organic semiconductors: aggregate emission in regioregular polythiophene. Phys Rev Lett 98(20):206406. https://doi.org/10.1103/PhysRevLett.98.206406